



# ING. MECATRÓNICA

**Tesis previa a la obtención del título de  
Ingeniero en Mecatrónica.**

**Autor:** Ing. Matias Stalin Checa Carranza

**Tutor:** Ing. Guillermo Mosquera

Diseño de una línea de termoformado para la producción de bandejas para  
huevos de codorniz

Design of a thermoforming line-process for production of quail  
egg trays

Quito-2026

## CERTIFICACIÓN DE AUTORÍA

Yo, Matias Stalin Checa Carranza declaro bajo juramento que el trabajo aquí descrito es de mi autoría; que no ha sido presentado anteriormente para ningún grado o calificación profesional y que se ha consultado la bibliografía detallada.

Cedo mis derechos de propiedad intelectual a la Universidad Internacional del Ecuador, para que sea publicado y divulgado en internet, según lo establecido en la Ley de Propiedad Intelectual, Reglamento y Leyes.



**Autor:** Matias Stalin Checa Carranza

**C.I.:**1725041568

## APROBACIÓN DEL TUTOR

Yo Guillermo Mosquera certifico que conozco a la autor/a del presente trabajo de titulación denominado "Diseño de una línea de termoformado para la producción de bandejas para huevos de codorniz", Matias Stalin Checa Carranza, siendo la responsable exclusivo/a tanto de su originalidad y autenticidad, como de su contenido.



DIRECTOR DEL TRABAJO DE TITULACIÓN

## ACKNOWLEDGMENTS

To my parents and family, who have been the unwavering foundation upon which I have built my life. Thank you for being the driving force behind my education and for tirelessly striving, through your example, to help me become a well-rounded individual. Your sacrifice and faith in me are the reason I have achieved this milestone today; this degree belongs to you.

To my classmates and friends, my brothers in this university journey. Thank you for every day we shared, for the lessons learned outside the classroom, and for pushing me to be a better version of myself when my strength faltered. Without your support, this journey would not have had the same meaning.

A deep and sincere thank you to my advisors, Eng. Guillermo Mosquera and Eng. Angélica Quito. Thank you for being fundamental guides in this process; your vast knowledge and your people skills transformed a complex challenge into a fascinating project. I admire not only their professional excellence, but also the human touch with which they guided me every step of the way.

To the geniuses and revolutionaries who have transformed our reality: Sam Altman, Mark Zuckerberg, and other pioneers like Warren McCulloch. Thank you for your vision and for the technological tools that today allow us to expand the boundaries of human knowledge. Artificial intelligence was not only a fundamental educational tool for understanding and effectively solving problems in this thesis, but also a source of inspiration for aspiring to one day be as influential in society as you are.

Finally, I thank myself, that inner strength and determination that, in moments of greatest doubt, reminded me that I could not abandon what I had started. Thank you to my willpower for remaining steadfast and for reminding me that excellence is not an act, but the habit of never giving up.

# CONTENTS

<b>1</b>	<b>INTRODUCTION</b>	<b>1</b>
<b>2</b>	<b>METHODOLOGY</b>	<b>12</b>
2.1	REQUIEREMENTS . . . . .	12
2.1.1	FUNCTIONAL REQUIREMENTS . . . . .	13
2.1.2	NON-FUNCTIONAL REQUIREMENTS . . . . .	13
2.1.3	CONSTRAINS . . . . .	13
2.2	CONCEPTUAL DESIGN . . . . .	14
2.3	SPECIFIC DESIGN . . . . .	17
2.4	MATERIAL SELECTION . . . . .	17
2.5	PRODUCT AND MOLD DESIGN . . . . .	18
2.5.1	Comparative Analysis and Mold Material Selection . . . . .	19
2.6	MECHANICAL AND PNEUMATIC DESIGN . . . . .	19
2.7	HEATING SYSTEM DESIGN . . . . .	22
2.8	VACUUM SYSTEM DESIGN . . . . .	23
<b>3</b>	<b>RESULTS</b>	<b>26</b>
3.1	THERMAL VALIDATION OF HEATING SYSTEM (SOLIDWORKS) . . . . .	26
3.1.1	Transient State Analysis and Heating Curves . . . . .	28
3.1.2	TEST 1 (Distance 65 mm - Cold Start) . . . . .	28
3.1.3	TEST 2 (Distance 40 mm - Cold Start) . . . . .	28
3.1.4	TEST 3 (PREHEATING) . . . . .	29
3.2	THERMOFORMING PROCESS SIMULATION(ANSYS) . . . . .	30
3.3	KINEMATIC AND SEQUENTIAL VALIDATION (UNITY 3D) . . . . .	31
3.3.1	Pneumatic Actuation Calculation . . . . .	32
<b>4</b>	<b>CONCLUSIONS AND RECOMMENDATIONS</b>	<b>35</b>
4.1	CONCLUSIONS . . . . .	35

4.2 RECOMMENDATIONS ..... 35

## LIST OF FIGURES

1.1	Thermoforming process using pressure method [1] . . . . .	2
1.2	Characteristic curves of the plant for different voltage levels (electrical resistance 200 W) [2] . . . . .	5
2.1	Stakeholder proposal prototype . . . . .	14
2.2	Own authorship Proposal #1 . . . . .	15
2.3	Own authorship Proposal #2 . . . . .	15
2.4	Flowchart of the process . . . . .	16
3.1	Steady state analysis . . . . .	27
3.2	PET Sheet and Heater temperatures at a distance of 65mm . . . . .	28
3.3	PET Sheet and Heater temperatures at a distance of 40mm . . . . .	29
3.4	PET Sheet and Heater temperatures with initial working temperature of Quartz elements . . . . .	29
3.5	Transient State Analysis . . . . .	30
3.6	PET Sheet thickness in vacuum forming . . . . .	32
3.7	Thermoforming machine sequence . . . . .	33

## LIST OF TABLES

2.1	Comparison of thermal properties for mold materials . . . . .	19
2.2	Technical specifications for DSNU cylinders (Diameters 8-20 mm) [3] .	21
2.3	Applications and vacuum levels [4] . . . . .	24
3.1	Mean surface temperature and power density for Standard FQE range [5]	27

## Chapter 1

### INTRODUCTION

Thermoforming has become a fundamental process in polymer transformation, enabling the conversion of viscoelastic plastic sheets into parts with high dimensional stability and defined mechanical properties. This technique is predominant in the food packaging industry, where not only physical containment but also hygienic preservation and visual appeal of the product are required.

In the specific context of quail egg packaging, the technical demands are heightened due to the need to guarantee the optical transparency of the material without compromising the structural integrity of the container. However, achieving these quality standards requires mastering critical variables such as uniform heat distribution and forming pressure, challenges that often necessitate automation solutions.

Thermoforming is a thermal forming process for plastic materials that transforms a thermoplastic sheet (semi-finished product) by heating it to a viscoelastic or viscoflexible state. In this phase, the material can be easily deformed by applying differential pressure (vacuum or positive pressure) and/or mechanical stretching, generally using a single mold (female or male mold) [6].

The process consists primarily of the following stages , as shown in Figure 1.1:

1. **Heating:** The plastic sheet is heated to the optimal molding temperature (generally within the tempering range). This heating can be achieved using electric resistance heaters (radiant heating elements), contact heating, hot air convection, infrared radiation, or a combination of these methods. Achieving uniform heat distribution is crucial to prevent unwanted deformation.
2. **Molding:** Once the material has reached the appropriate temperature, molding is carried out using a thermoforming tool. This process can be performed by vacuum, positive pressure, plug-assisted forming, or combinations of these

techniques, depending on the level of detail, depth, and complexity of the final part.

3. **Cooling:** After molding, the material must be cooled inside the mold until it reaches a temperature at which the part becomes intrinsically stable. This process can be passive (by conduction with the mold) or active (cooling by forced air or water circulation in the mold). Controlled cooling is essential to minimize internal stresses and subsequent deformations.
4. **Demolding:** Once cooled, the part is removed from the mold. Demolding can be done manually or automatically, and can be assisted by reverse vacuum, mechanical systems, or compressed air, depending on the mold design and the forming method used.

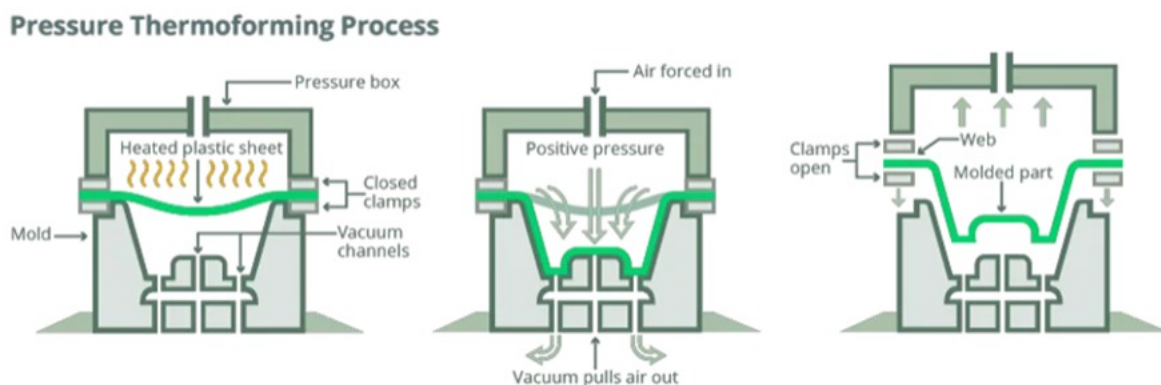


**Figure 1.1.** Thermoforming process using pressure method [1]

As mentioned in the PLASTIGLAS [7] thermoforming technical manual, all thermoplastic polymers are suitable for the thermoforming process. When heated, these materials exhibit variations in their modulus of elasticity, hardness, and load-bearing capacity. Therefore, one of the critical aspects of the thermoforming process is the correct selection and control of the temperature applied to the plastic material. It is essential that, regardless of the heat transfer method used, the plastic sheet reaches the optimal thermal range known as the tempering range. Furthermore, it is crucial to ensure uniform heating across the entire surface of the material to guarantee proper shaping .

However, in practice, accurately measuring the actual temperature of the sheet can be complex, even when using contact thermometers. For this reason, temperature assessment is generally based on the physical behavior of the material during heating. One of the most commonly used indicators is the point at which the sheet begins to gradually deform, which indicates that the ideal molding temperature has been reached [7]. For more precise control, it is essential to use the correct instrumentation for the designated variable. In their work [8], they highlighted the TM4 temperature controllers as an option, as they replaced the CH402 modules because they feature RS485 communication, allowing their integration with the HMI and PLC. They also recommend Type K thermocouples, which are useful for the established temperature range (-200 °C to 0 °C \* 0 °C to 1250 °C) in thermoforming processes. On the other hand, in his thesis Miranda [9], he mentions that the cooling process is crucial in the manufacturing process, as it directly influences the quality of the finished product. The optimal temperature for demolding is approximately 10 °C below the material's deflection temperature under load.

For heating methods and heat sources, one of the most widely used technologies is the electric resistance oven, which uses electricity as an energy source to generate heat in a heating chamber. This operation is based on the Joule effect, according to which an electric current flowing through a resistive conductor causes heat generation. [10] A typical electric oven consists of a heating chamber, heating elements (electric resistance elements), thermocouples for temperature measurement, insulating material to reduce heat loss, a timer, and an electronic controller that regulates the power and heating time. The efficiency of this system depends directly on the quality of the heating elements and the thermal control implemented.

I. Morán and B. Laica [11] assert that the use of electric resistance ovens makes the process efficient, durable, and environmentally friendly. In their project, they developed an electric resistance oven with a nominal power of 1200 W and a supply voltage of 220–240 V. This equipment integrated a power control system into the heating elements, allowing for controlled and precise temperature variation. Furthermore, it

incorporated sensors to provide feedback to the system and a control panel that gave the operator the ability to monitor and adjust the thermal process in real time, thus optimizing energy efficiency and operational safety.

An essential component in these systems is the tubular metal heating element, composed of three main elements:

- Tubular metal sheath: made of materials such as INCOLOY, stainless steel, copper, or special alloys, it provides mechanical strength and protection
- Electrical insulating material: generally high-purity magnesium oxide, which, in addition to electrically insulating the conductor, offers high thermal conductivity against oxidation.
- Helical resistive wire: made of high-resistivity alloys, it is the element responsible for heat generation [11].

In this type of heating element, the wire is the heat generator; the magnesium oxide acts as an efficient thermal interface between the resistive wire and the metal sheath, ensuring rapid and homogeneous heat transfer. Tubular metal heating elements are notable for their compactness, durability, and adaptability to different configurations, and are widely used in heating air, liquids, oils, surfaces, ovens, and drying cabinets [12].

As mentioned previously automation and precision in thermal control are determining factors in the quality of thermoforming. In certain industrial systems, infrared radiation heaters combined with optical sensors are used to detect in real time the yield point or controlled buckling of the plastic sheet. This phenomenon, which indicates the arrival of the optimal forming temperature, is identified by photoelectric cells [7]. Once detected, the system can automatically adjust the exposure time or the power supplied, thus ensuring that the material remains at optimal thermal conditions.

In the research developed by Rosales-Dávalos et al. [2], a closed-loop temperature control system (CLTSS) was designed and implemented for the thermoforming of blocks manufactured from post-consumer multilayer packaging. Process control was

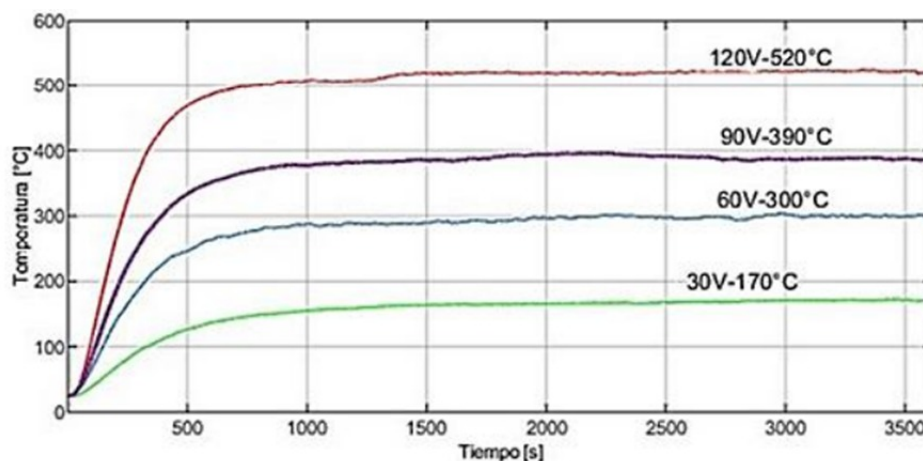


**Figure 1.2.** Characteristic curves of the plant for different voltage levels (electrical resistance 200 W) [2]

based on obtaining a mathematical model of the plant from experimental data and analysis in Matlab, considering a 120 VAC power supply. The results obtained in Figure 1.2 was a first-order transfer function, which was then tuned using the Ziegler-Nichols method for a PID controller.

The control architecture included the reference input, the controller block, the power stage, the heat exchanger, and a feedback loop. This design allowed the resistor temperatures to be maintained within a narrow stability range, preventing overheating and significant temperature fluctuations.

The results demonstrated that the PID system exhibited a more stable response than the ON/OFF control, with smaller oscillation amplitudes and faster convergence to the target temperature. This improvement translates into a more uniform thermoforming process, which is especially relevant in applications where thermal accuracy is critical to the final product quality.

In the field of thermoforming of plastic materials, the selection of the forming system is crucial for achieving the desired quality and characteristics in the final product. Tupia et al. [13] propose compression molding as an economical alternative for recycling thermoplastics mixed with wood (in a ratio of 70% plastic and 30% wood), achieving the manufacture of simple geometry parts with a uniform surface finish. The process is carried out by heating the material to 190°C for 55 minutes, then applying a compression force of 34 kN to the mold, ending with a controlled cooling period of 10 minutes.

The application of these parameters resulted in the production of high-quality plastic panels with consistent mechanical properties and surface finish, a product of the alloy of the raw material with wood. This can be beneficial for protecting and storing more fragile items with a high probability of damage.

In another study, González-Bernal et al. [14] emphasize that, for the design of a hydraulic press intended for thermoforming, it is essential to conduct a prior analysis of the pressure and temperature conditions required to correctly deform the material. They determined that the mold should reach 240 °C and that the necessary closing force was 676 kN. These conditions imply the use of structural materials capable of withstanding high loads and temperatures, as well as meeting the mechanical strength and durability standards required in an industrial environment.

On the other hand, in the context of packaging transparent products, the specialized literature indicates that maintaining transparency is a challenge, since thermoforming can reduce the optical clarity of the material. To minimize visual distortions, it is crucial to optimize the mold's surface finish, the strategic placement of vent holes, and the structural reinforcement of the cavities [15]. While vent holes are essential for removing trapped air during forming, their placement should avoid visible areas of the container. Furthermore, rougher mold surfaces promote airflow but negatively affect transparency, necessitating a balance between visibility and the efficiency of the ventilation process. This aspect is particularly relevant to the present research, as quail egg trays are intended for the food industry, where a high level of hygiene, visual quality, and functionality is required. An optimized mold design not only ensures a more attractive presentation for the consumer but also contributes to maintaining the integrity and optimal preservation of the packaged product.

In the development of industrial machinery, compliance with technical standards and safety codes not only guarantees design quality but also facilitates subsequent implementation and commercialization. In the context of this thermoforming machine project for quail egg cartons, the adoption of national and international standards has ensured that the prototype meets the mechanical, thermal, hygiene, and safety requirements

established for the food industry. The main applicable standards and their relevance in similar projects are summarized below [10] [16]:

- NTE INEN 1373: Ecuadorian technical standard that defines the general requirements that thermoforming and injection systems must meet. Its application ensures that the design complies with national manufacturing and assembly standards, especially regarding dimensional accuracy and safe operation.
- ISO 6259-2: Establishes methods for conducting tensile tests on thermoplastic sheets. In the virtual design, these values can be used as a reference in simulations of the sheet's mechanical resistance during thermoforming.
- ISO 6259-2: Establishes methods for performing tensile tests on thermoplastic sheets. In the virtual design, these values can be used as a reference in simulations of the sheet's mechanical resistance during thermoforming.
- ISO 11607:2019: Specifies the requirements for thermoformable packaging materials and processes intended to maintain sterility, which is relevant for food packaging and products with high sanitary standards.

An interesting proposal to strengthen this code was developed in article [17], which presents a CNN-based approach designed for quality control of the sealing and closure of thermoformed containers. Using a practical case study in a real-world industrial setting, the main components to consider for design are detailed; the designed machine vision system and the image-based criteria defined to determine when a product should be accepted or rejected are presented.

- BS EN 12409:2008: European standard that regulates the assembly of thermoforming machines.
- ASTM E659: Determines the auto-ignition temperature of materials exposed to high temperatures. This information can be integrated into thermal modeling to prevent combustion risks in the process. In the virtual validation phase, these standards provide technical parameters that can be incorporated as constraints

and evaluation criteria in CAD models, finite element simulations (FEM), and thermal analyses. Subsequently, in the physical construction phase, they can serve as a reference for material selection, process configuration, and verification and testing procedures.

In the virtual validation phase, these standards provide technical parameters that can be incorporated as constraints and evaluation criteria in CAD models, finite element simulations (FEM), and thermal analyses. Subsequently, in the physical construction phase, they can serve as a reference for material selection, process configuration, and verification and testing procedures.

According to the scope of this thesis, the use of computer-aided design (CAD) tools and digital twin technologies represents a key strategy for optimizing thermoforming processes before their physical implementation. A digital twin, fed with data from sensors and programmable logic controllers (PLCs), allows for the accurate modeling of machine operating parameters, anticipating problems and reducing production costs. According to Turan et al. [18], this methodology has demonstrated significant improvements in industrial key performance indicators (KPIs), decreasing the waste rate by 50% and raw material consumption by 10%, resulting in substantial cost savings.

In this approach, finite element simulations (FEM) and data analysis play an essential role. The Neo-Hookean (NH) model, combined with the Williams-Landel-Ferry (WLF) approximation, is particularly useful for representing the mechanical and thermal behavior of temperature-dependent materials, allowing for the accurate simulation of thermoplastic sheet performance during heating and forming [18]. This predictive capability is fundamental for establishing temperature and time settings before physically constructing the thermoforming machine.

Cortez et al. [19] emphasize that the feasibility of a machine design depends on prior mechanical modeling that considers real materials, shapes, and dimensions. In their research, 3D modeling allowed for the optimization of both the structure and ergonomics of the equipment. Similarly, for the present project, the use of software such as SolidWorks/Inventor will facilitate the structural analysis of the frame, the thermal

distribution in the oven, and accessibility for the operator.

Other studies demonstrate the versatility of CAD modeling in diverse industrial applications. For example, in [20], a conceptual model of a graphene flash synthesis system was developed, capable of transforming carbon-rich waste (such as plastics, coconut shells, or tires) into high-quality graphene, using SolidWorks to validate the structural and functional viability of the prototype. In the "LegnAttivo" project [21], Computational Design (CD) and Design for Fabrication (DfM) techniques were applied to the construction of prefabricated facades, achieving time and cost reductions through digital manufacturing strategies. These experiences demonstrate that the integration of CAD with manufacturability criteria can be transferred to the design of the thermoforming machine, optimizing mold construction, sheet clamping, and displacement mechanisms.

The simulation of external conditions is also a valuable resource. In a study comparing two types of wind turbines using SolidWorks, their performance was analyzed at different wind speeds by visualizing streamlines. Simulations were performed on each type at varying wind speeds (0.5–4.5 m/s). A Savonius simulation was initiated, and the airflow over the blades was studied using streamlines. The vertical speed of a blade was determined using the cut plot command [22]. This approach is applicable to the present work, as factors such as air currents or forced ventilation can influence heat dissipation and, consequently, the quality of the thermoforming process.

Furthermore, the thermal and mechanical behavior of thermoformable materials can be evaluated using studies such as the one presented in [23], where polymeric syntactic foams (PSF) were analyzed under compressive and tensile loads within a temperature range of 25 °C to 100 °C. The results showed a notable decrease in compressive strength with increasing temperature, a phenomenon that must be considered when defining the operating thermal profile. In our case, this type of analysis would allow us to select materials that maintain dimensional stability and adequate mechanical properties even under prolonged operating conditions or in environments with significant thermal variations.

In short, the implementation of CAD models with FEM simulations and digital twin prin-

ciples will allow us to virtually validate the design of the thermoforming machine, optimize material consumption, anticipate structural or thermal failures, and ensure that the prototype meets performance, safety, and quality requirements before its physical manufacturing. This work seeks to strengthen these models by expanding them to a more complex level, since the current state of the prototypes and designs presented by the researchers does not include a comprehensive didactic simulation of the process that demonstrates an automated process.

The development of an automated thermoforming system for quail egg packaging is justified by the urgent need to modernize production processes within the agro-industrial sector. Currently, small-scale producers rely on manual or semi-automated methods that result in non-standardized and fragile containers, failing to meet modern consumer expectations regarding safety, hygiene, and durability. This project addresses these deficiencies by transitioning from manual control to a robust automated system, thereby solving critical issues such as material deformation, structural instability, and high waste rates caused by inconsistent heating and lack of synchronization. From an industrial perspective, this project is vital for the strategic expansion of MAR-ALTO. By implementing this production line, the company will not only enhance its competitiveness and revenue but will also provide a scalable solution for small agricultural entrepreneurs. This technology transfer allows these stakeholders to access competitive markets with high-quality products, overcoming the limitations of current packaging that restrict their growth and marketability.

Finally, the academic contribution of this thesis lies in the practical application of industrial automation to solve real-world manufacturing inefficiencies. It serves as a model for sustainable manufacturing solutions, demonstrating how advanced control systems can optimize resource usage and reduce production errors in niche industries. This project not only bridges the gap between manual and automated manufacturing but also fosters technical skill development in a key engineering area.

The main objective is to automate the thermoforming and shaping process of plastic quail egg trays through the implementation of an integrated production system that

optimizes material displacement, controlled heating, sheet forming, and vacuum molding.

To fulfill the main objective we are going to focus on:

- Develop the mechanical and control architecture required for synchronized advancement of the plastic sheet, incorporating limit switches, pneumatic actuators, and a state-based control strategy.
- Integrate a heating subsystem equipped with temperature sensors to ensure uniform and stable heating of the PET sheet.
- Engineer an efficient vacuum system capable of generating the required negative pressure for proper molding of the quail egg trays, ensuring adequate sealing, suction timing, and mold performance.
- Conduct functional tests and performance evaluations to verify thermal stability, vacuum quality, and final product conformity according to the design specifications.

## **Chapter 2**

### **METHODOLOGY**

The development methodology is based on the VDI 2206 standard, applying the "V" lifecycle to ensure interdisciplinary integration between the mechanical, electronic, and computer domains. The process begins with defining requirements and design parameters based on the rheological properties of polyethylene terephthalate (PET) and the morphometry of the egg, which allows for establishing the system's functional constraints. Subsequently, domain-specific design is performed, involving mathematical modeling and dimensioning of thermal, mechanical, and vacuum loads, followed by component selection according to energy efficiency. Finally, the methodology includes system integration and virtual validation using CAD/CAE tools, fulfilling verification cycles that guarantee product integrity against the initially established technical requirements.

#### **2.1. REQUIEREMENTS**

The initial phase of the top-down branch of the model focuses on the comprehensive definition of requirements, which form the basis for the conceptual design and subsequent validation of the mechatronic system. In this project, the list of technical specifications was consolidated through a concurrent engineering process developed in direct collaboration with industry stakeholders, ensuring that the design meets the real needs of the target market. To determine the machine's geometric and functional constraints, a detailed analysis of quail egg morphometry and the rheological properties of polyethylene terephthalate (PET) was integrated. This approach allowed the translation of business objectives into measurable technical parameters, guaranteeing that the production of egg cartons meets the quality, efficiency, and technical feasibility standards required in the production environment.

### **2.1.1. FUNCTIONAL REQUIREMENTS**

- The system shall raise the temperature of the PET sheets to the thermoforming range, between 120°C and 140°C.
- The machine must guarantee a minimum production rate of one tray per minute.
- The system must be capable of forming trays designed to hold between 12 and 24 quail eggs.
- An alarm system must be integrated to notify of critical errors, along with an easily accessible emergency stop button for immediate process shutdown by the operator.

### **2.1.2. NON-FUNCTIONAL REQUIREMENTS**

- The system must process food-grade certified PET plastic sheets, ensuring the safety of the final product.
- The mold holder design shall allow die changes to accommodate different tray formats without requiring structural modifications to the machine.
- The mechanical design must prioritize accessibility to critical components and clearly define lubrication points to facilitate preventive and corrective maintenance.

### **2.1.3. CONSTRAINS**

- The entire production line(machine) must be confined within a maximum plant area of 3 m<sup>2</sup>.
- All components in direct or indirect contact with the packaging must feature smooth, easily sanitizable surfaces. The following material specifications are Stainless Steel (AISI 304/316) and Aluminum Alloys.

- The system must operate while maintaining minimal noise levels to ensure a safe and ergonomic working environment for the operator following the ISO 9612.

## 2.2. CONCEPTUAL DESIGN

In this phase, the design alternatives for the thermoforming system were analyzed, evaluating the material feeding efficiency and the mechanical complexity of each proposal. Three main proposals were evaluated based on the automation requirements and the control of critical variables such as temperature and time.

**Proposal 1 (Roll Feed):** This alternative, initially suggested by the stakeholders in Figure 2.1, consisted of a continuous supply of plastic via a roll feeding a conveyor belt. While it allowed for a constant flow, it presented critical difficulties in maintaining uniform tension on the 1 mm thick PET sheet and risks of material deformation due to thermal variations in the pre-forming stages.

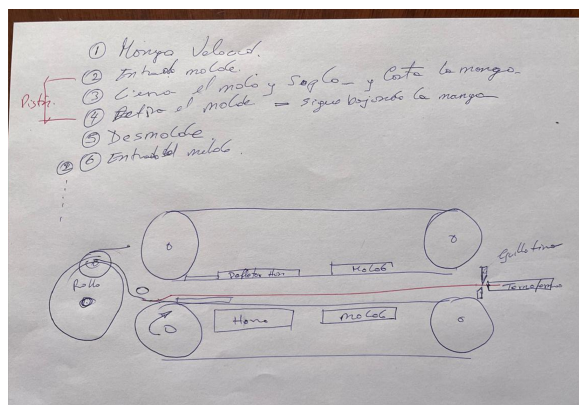


**Figure 2.1.** Stakeholder proposal prototype

**Proposal 2 (Piston-Rack System):** This proposal sought to automate the movement using precision mechanisms as shown in Figure 2.2. However, the integration of this system increased the mechanical complexity and cost of the prototype without resolving the problem of handling thin sheets.

**Proposal 3 (Compact):** Figure 2.3 show an integrated vertical displacement architecture system, consolidating the heating, thermoforming, and cooling stages into a small area. While this model significantly optimized space utilization in the production plant, it lacked an automated mechanism for supplying PET sheets.

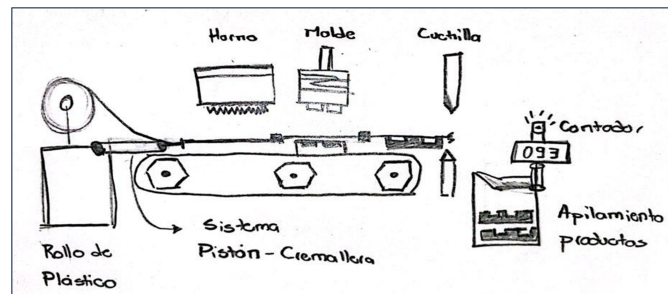


**Figure 2.2.** Own authorship Proposal #1

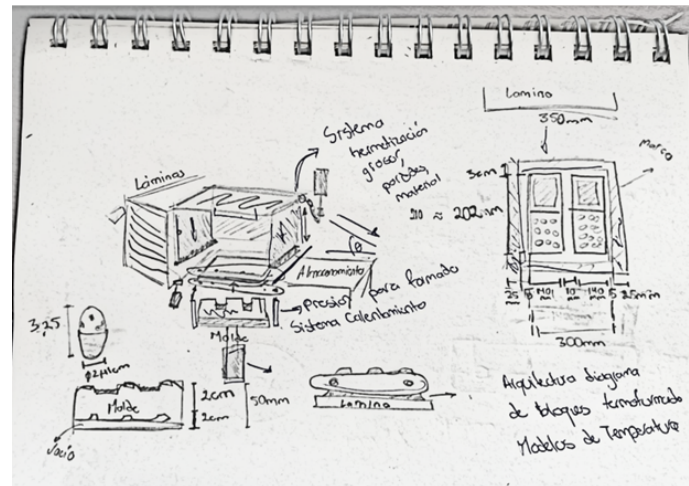


**Figure 2.3.** Own authorship Proposal #2

Despite this initial limitation, this proposal laid the groundwork for the development of the final design. It was determined that, since removing the formed part requires mandatory operator intervention at the end of each cycle, integrating a fully automated sheet feeder would result in an oversized technical and economic footprint for the prototype.

For this reason Figure 2.4 provides a graphical representation of the process and stages that were finally decided. Highlighting the main steps as sheet feeding by operator, the movement system, heating and vacuum forming and the extraction of the mechanized sheet by user.

Under this design approach, the operator can insert the new sheet as a sequential task immediately following the removal of the finished product. This approach allows for maintaining the required production times and simplifying the mechanical complexity of the system, limiting human intervention to minimal and critical stages of the process that ensure workflow continuity.

The operational logic of the thermoforming machine is structured into four main sequential stages, integrated with a centralized safety system. Figure 2.4 provides a graphical representation of the workflow and the interaction between the mecatronic sub-systems.

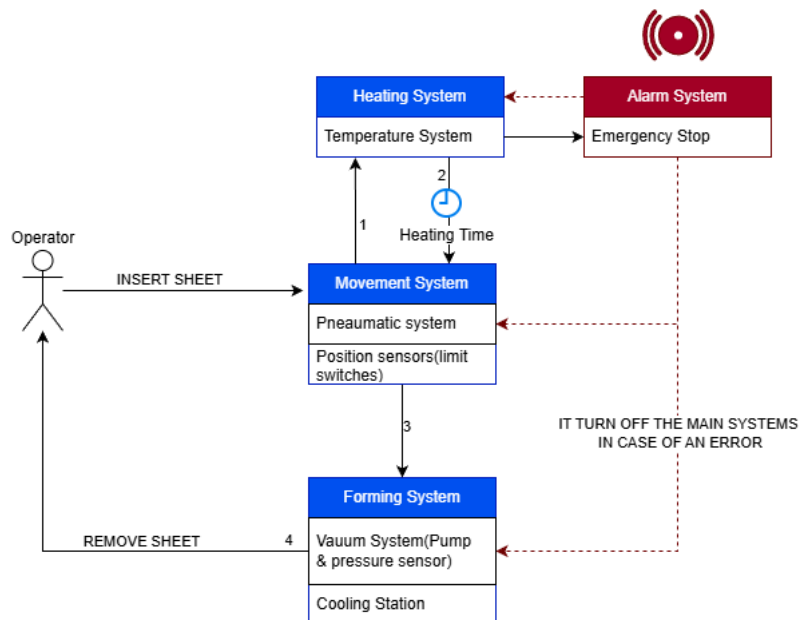


**Figure 2.4.** Flowchart of the process

**Stage 1:** The cycle begins with the operator manually inserting the thermoplastic sheet into the movement system. This stage relies on human intervention to ensure proper alignment before the pneumatic clamping and positioning take place.

**Stage 2:** Once the sheet is positioned, the heating system is activated. The system monitors the Heating Time parameter to reach the polymer's molding temperature, ensuring optimal material malleability for the forming process.

**Stage 3:** Upon completion of the heating cycle, the movement system driven by pneumatic actuators transfers the sheet to the forming station. This displacement is monitored by position sensors (limit switches) to guarantee precise mechanical alignment.

**Stage 4:** The forming system initiates the vacuum sequence using a pump and a pressure sensor to ensure the sheet conforms strictly to the mold geometry. After a stabilization period in the cooling Station, the cycle concludes, and the operator removes the finished part.

### 2.3. SPECIFIC DESIGN

Once the conceptual architecture based on manual sheet feeding was defined, the specific design focused on the detailed engineering of each subsystem. The main objective was to integrate the stages of raw material supply, heating, vacuum forming, and cooling. This design ensures rigorous control of critical variables such as softening temperature and cycle times, guaranteeing that the final product meets the structural rigidity standards for consumer goods storage.

### 2.4. MATERIAL SELECTION

To justify the selection of the raw material, a comparison was made between the three most common polymers in the thermoforming industry for food packaging: Polyethylene Terephthalate (PET), High Impact Polystyrene (HIPS), and Polyvinyl Chloride (PVC).

- PET (Polyethylene Terephthalate): Selected for its high transparency, mechanical strength, and 100% recyclability<sup>2</sup>. It maintains a stable thermal window between  $120^{\circ}C$  and  $140^{\circ}C$ .
- HIPS (High Impact Polystyrene): Although it is easier to thermoform due to low thermal shrinkage, its lack of transparency makes it unsuitable for quail egg trays, where product visibility is a commercial requirement.
- PVC (Polyvinyl Chloride): Despite its low cost, it was discarded due to the emission of toxic gases during heating and its lower environmental sustainability compared to PET.

The material selected after the initial analysis was PET plastic, widely used in the food industry and valued for its excellent surface finish and post-processing structural rigidity. A roll 1 mm thick and 350 mm wide was chosen; these dimensions served as the basis for the structural sizing and design of the rest of the machine's components.

Among its most outstanding technical properties are high stability and rigidity, good abrasion and tear resistance, and favorable sliding characteristics. The material also offers chemical resistance to dilute acids, aliphatic and aromatic hydrocarbons, oils, greases, and alcohols. It is weather-resistant and has good electrical insulation properties.

It was proposed that the roll be segmented into sheets 350mm x 270mm long, with the aim of placing a die that can mold two egg trays on a single sheet (placed parallel to each other), each tray would have a maximum storage capacity of 15 quail eggs, which would fall within the required product range in one tray.

## 2.5. PRODUCT AND MOLD DESIGN

The design of the mold constitutes a critical stage that bridges the product's physical requirements with the mechanical capabilities of the vacuum thermoforming process. The mold design utilized the average dimensions of the product as a primary reference, based on studies reporting an average longitudinal diameter of  $22.35 \pm 0.06$  mm. Priority was given to a geometry that optimizes the vacuum thermoforming process, ensuring a balance between production speed and structural integrity. In accordance with established industrial standards for thermoplastic processing, the following fundamental geometric characteristics were incorporated:

- **Draft Angle:** A draft angle between  $3^\circ$  and  $5^\circ$  was implemented on all vertical walls to facilitate efficient part release.
- **Transition Radii:** Generous radii were applied at transitions and corners to ensure uniform material distribution and prevent localized thinning.
- **Edge Optimization:** Sharp edges and pronounced right angles were avoided to mitigate the risk of material tearing during the high-speed demolding phase.

The resulting convex profile of the mold aligns with the natural morphology of the quail egg, which inherently facilitates the release of the PET sheet after the cooling stage.

### 2.5.1. Comparative Analysis and Mold Material Selection

The thermodynamic performance of the mold is essential for maintaining a high production rate. While stainless steel was initially considered for its hygienic properties, **6061-T6 Aluminum Alloy** was selected for the manufacturing of the mold block. This decision is justified by the critical difference in thermal conductivity,

**Table 2.1.** Comparison of thermal properties for mold materials

Material	Thermal Cond. ( $W/m \cdot K$ )	Impact on Production Cycle
AISI 304 Stainless Steel	$\approx 16$	Slow heat dissipation; extended cycle times.
<b>6061-T6 Aluminum</b>	$\approx 167$	Rapid solidification; high efficiency.

The high thermal conductivity of aluminum allows the PET sheet to dissipate heat rapidly, enabling the polymer to solidify in significantly reduced times. This property ensures an efficient production cycle without requiring complex active cooling systems. To satisfy food safety (FDA) requirements and ensure wear resistance, the aluminum mold undergoes a **hard anodizing** surface treatment. This coating provides a non-porous ceramic surface that is easy to clean and possesses high surface hardness, eliminating risks of contamination and corrosion.

For the **clamping frame** and perimeter support, **AISI 304 Stainless Steel** is utilized. Its austenitic structure provides excellent corrosion resistance to ambient humidity and cleaning agents (CIP processes). This material is ideal for structural components that require indirect food contact, ensuring a hygienic and durable production environment.

## 2.6. MECHANICAL AND PNEUMATIC DESIGN

The pneumatic actuation mechanism is designed to raise and lower the mounting frame and the PET sheet during the forming cycle. The design incorporates two cylinders operating in parallel to ensure balanced movement and prevent structural stick-slip phenomena.

## Load Estimation (Static Analysis)

The masses of the moving components were calculated using the physical properties from the Autodesk Inventor software. The density of **AISI 304 Stainless Steel** ( $\rho \approx 8 \text{ g/cm}^3$ ) was used for all structural elements, prioritizing hygiene and corrosion resistance throughout the assembly.

- Moving Base Frame Mass ( $M_{base}$ ): 0.972 kg
- Clamping Frame Mass ( $M_{clamp}$ ): 1.024 kg
- PET Sheet Mass ( $M_{PET}$ ): 0.146 kg

The total mass to be displaced ( $M_T$ ) and the total weight ( $W_T$ ) are defined as follows:

$$M_T = \sum m_i = 0.972 + 1.024 + 0.146 = 2.142 \text{ kg} \quad (2.1)$$

$$W_T = M_T \cdot g = 2.142 \text{ kg} \cdot 9.81 \text{ m/s}^2 \approx 21.01 \text{ N} \quad (2.2)$$

## Design Force and Safety Factor

To compensate for dynamic seal friction, pressure losses in pneumatic lines, and to ensure adequate acceleration ( $\eta \approx 80\%$ ), a Safety Factor ( $S_f$ ) of 1.4 was applied.

$$F_{req} = W_T \cdot S_f = 21.01 \text{ N} \cdot 1.4 \approx 29.41 \text{ N} \quad (2.3)$$

Given that the load is symmetrically distributed between two actuators, the required force per cylinder is:

$$F_{cyl} = \frac{F_{req}}{2} = 14.71 \text{ N} \quad (2.4)$$

## Piston Diameter Selection

Considering a standard industrial line pressure of  $P = 4 \text{ bar}$  (0.4 MPa), the required effective area ( $A_{req}$ ) is calculated as:

$$A_{req} = \frac{F_{cyl}}{P} = \frac{14.71 \text{ N}}{400,000 \text{ Pa}} = 3.68 \times 10^{-5} \text{ m}^2 \quad (2.5)$$

The theoretical diameter ( $D_{teo}$ ) required is:

$$D_{teo} = \sqrt{\frac{4 \cdot A_{req}}{\pi}} \approx 6.84 \text{ mm} \quad (2.6)$$

Although the theoretical calculation suggests a minimum diameter of  $\approx 7$  mm, the final selection is constrained by the required operating stroke of **200 mm**. Under the **ISO 6432** standard for micro-cylinders, smaller diameters (8 mm or 10 mm) are generally not manufactured with such long strokes due to the critical risk of rod **buckling** under load. The smallest standard commercial diameter that guarantees structural stability for a 200 mm stroke is 12 mm.

**Table 2.2.** Technical specifications for DSNU cylinders (Diameters 8-20 mm) [3]

<b>Piston [mm]</b>	<b>8</b>	<b>10</b>	<b>12</b>	<b>16</b>	<b>20</b>
Conforms to standard	ISO 6432				
Pneumatic connection	M5			G1/8	
Piston rod thread	M4	M6		M8	
Stroke [mm]	1 ... 100	1 ... 200	1 ... 320		
Design structure	Piston / piston rod / cylinder barrel				
<b>Cushioning</b>					
DSNU-...-P	Elastic cushioning rings/plates at both ends				
DSNU-...-PPV	–	Adjustable cushioning at both ends			
DSNU-...-PPS		–	Self-adjusting cushioning		
<b>Cushioning length [mm]</b>					
DSNU-...-PPV	–	9	12	15	
DSNU-...-PPS		–	12		
Position detection	For proximity sensor				
Type of mounting	Direct mounting (only MH variant) / With accessories				
Mounting position	Any				

This actuator generates an advance force of 45.2 N at 4 bar, significantly exceeding the required force (14.71 N), thus validating its functional and mechanical suitability.

## 2.7. HEATING SYSTEM DESIGN

The thermal conditioning stage is critical to ensure the plasticity of the PET sheet without degrading its optical properties or mechanical strength. The system is designed to raise the polymer temperature from room temperature (25 °C) to the glass transition and forming range (115 °C - 140 °C) within a controlled cycle. Based on the thermo-physical properties of polyethylene terephthalate (PET) [24], and the dimensions of the sheet to be processed, the energy required for the phase change was determined.

- Specific Heat Capacity of PET ( $C_p$ ):  $\approx 1300 \text{ J}/(\text{kg} \cdot ^\circ \text{C})$
- Sheet Mass ( $m$ ): 0.146 kg
- Target Temperature Rise ( $\Delta T$ ): 95 °C (considering a thermal jump from 25 °C to 120 °C)

The required heat energy ( $Q_{PET}$ ) is calculated using the fundamental calorimetry equation:

$$Q_{PET} = m \cdot C_p \cdot \Delta T \quad (2.7)$$

$$Q_{PET} = 0.146 \text{ kg} \cdot 1300 \frac{\text{J}}{\text{kg} \cdot ^\circ \text{C}} \cdot 95^\circ \text{C} \approx 18,047 \text{ J}$$

### Power Sizing

To meet the functional requirement of producing one tray per minute, a maximum heating time ( $t$ ) of 30 seconds was established, leaving the remainder of the cycle for forming, cooling, and ejection stages. The theoretical power ( $P_{theo}$ ) required is:

$$P_{theo} = \frac{Q_{PET}}{t} = \frac{18,047 \text{ J}}{30 \text{ s}} \approx 601.57 \text{ W} \quad (2.8)$$

Since infrared radiation heating involves significant losses due to convection to the surrounding air and dispersion of radiation not absorbed by the material, a Safety

Factor ( $S_f$ ) of 2.0 was applied. This safety margin also provides operational flexibility to process thicker gauge sheets in future applications.

$$P_{total} = P_{theo} \cdot S_f = 601.57 \text{ W} \cdot 2.0 \approx 1203 \text{ W} \quad (2.9)$$

### Heater Selection

To ensure uniform heat distribution over the effective working area (350 mm × 270 mm) and avoid the formation of "cold spots" that result in uneven thickness in the final product, a modular configuration of medium-wave ceramic infrared elements (FQE - Full Quartz Elements) was selected.

- **Configuration:** 4 quartz/ceramic heating elements of 400 W each, arranged equidistantly over the molding area.
- **Total Installed Power:**  $4 \times 400 \text{ W} = 1600 \text{ W}$ .

The installed power (1600 W) exceeds the design requirement (1203 W), ensuring that the system reaches the set-point temperature within the stipulated time without needing to operate the elements at 100% capacity, which significantly extends the lifespan of the resistors.

## 2.8. VACUUM SYSTEM DESIGN

The final forming stage uses negative pressure to mold the heated PET sheet against the die. The goal is to achieve a "low vacuum" level, as the packaging application does not require the microscopic level of detail demanded in other high-precision industries. It should be noted that any pressure below standard atmospheric pressure (101.325 kPa or 760 Torr) is considered a vacuum. For this design, the reference parameters are established using inches of mercury (inHg), a traditional unit representing the pressure exerted by a one-inch column of mercury at 0°C. Commonly used in North America and in the HVAC(Heating, Ventilation, and Air Conditioning) sector, inHg measures

**Table 2.3.** Applications and vacuum levels [4]

Vacuum level	Pressure (Torr)	Pressure (Pa)	Molecules / $m^3$	Applications
Atmospheric pressure	760	101.3 kPa	$2.5 \times 10^{25}$	Standard environment
Low vacuum (rough)	25 – 760	3 kPa – 100 kPa	$8.1 \times 10^{23}$ – $2.5 \times 10^{25}$	Material handling, packaging
Medium vacuum	$10^{-3}$ – 25	100 mPa – 3 kPa	$3.2 \times 10^{19}$ – $8.1 \times 10^{23}$	Scientific experiments
High vacuum	$10^{-9}$ – $10^{-3}$	100 nPa – 100 mPa	$3.2 \times 10^{13}$ – $3.2 \times 10^{19}$	Semiconductor manufacturing, electron microscopes
Ultra-high vacuum (UHV)	$10^{-12}$ – $10^{-9}$	100 pPa – 100 nPa	$3.2 \times 10^{10}$ – $3.2 \times 10^{13}$	Particle accelerators, surface science
Extremely high vacuum	$< 10^{-12}$	$< 100$ pPa	$< 3.2 \times 10^{10}$	Space simulation, advanced research

vacuum as a differential pressure relative to the atmosphere, where an absolute vacuum corresponds to 29.92 inHg at sea level [4]. It is crucial to consider the theoretical limit of the process: the maximum force that compresses the plastic against the mold is the weight of the atmosphere itself (14.7 psi or 1 bar). Regardless of the power of the selected pump, it is physically impossible to exert a forming force greater than this value; therefore, pump sizing focuses on the evacuation speed (flow rate) and not on exceeding this limiting force.

### Design Parameters

To size the pump flow rate, the total volume to be evacuated and the maximum allowable time within the production cycle were considered.

- **Volume to Evacuate ( $V$ ):** 0.1984 L (Sum of mold cavity and hose internal volume).
- **Initial Pressure ( $P_{init}$ ):** 1000 mbar abs (Standard atmospheric).
- **Target Pressure ( $P_{final}$ ):** 31.15 mbar abs (Equivalent to  $\approx 29$  inHg, considered optimal for PET thermoforming).
- **Evacuation Time ( $t$ ):** 1.5 seconds.

### Suction Flow Rate Calculation

The required volumetric flow rate ( $S$ ) is determined using the pump-down equation:

$$S = \frac{V}{t} \cdot \ln \left( \frac{P_{init}}{P_{final}} \right)$$

$$S = \frac{0.1984 \text{ L}}{1.5 \text{ s}} \cdot \ln \left( \frac{1000}{31.15} \right) \approx 0.459 \text{ L/s} \quad (2.10)$$

$$S \approx 1.65 \text{ m}^3/\text{h}$$

Based on the calculated minimum flow rate, a rotary vane vacuum pump was selected.

- **Selected Equipment:** Vacuum Pump with 1.2 CFM capacity (2.04 m<sup>3</sup>/h).
- **Oversizing Margin:**

$$\text{Margin} = \frac{2.04 - 1.65}{1.65} \approx 23.6\% \quad (2.11)$$

This 23% capacity margin ensures the mold reaches the target negative pressure in 1.5 seconds or less, compensating for potential minor seal leaks.

To optimize performance and automate the cycle, two auxiliary components are integrated:

1. **Vacuum Reservoir (Surge Tank):** Essential for absorbing instantaneous air demand during valve opening. The volume of the storage tank should be 2.5 times greater than the volume between the mold, the vacuum box, and the tubing [7].
2. **Absolute Pressure Transducer:** This sensor measures the actual pressure inside the cavity relative to a perfect vacuum. It provides a standard analog signal (4-20 mA) to the PLC, allowing precise automation of the vacuum cycle and fault detection.

## Chapter 3

### RESULTS

To verify the analytical design parameters and ensure the functionality of the thermoforming machine's operating cycle, a computational validation strategy was implemented, divided into three domains: thermal analysis of the heating chamber, rheological simulation of the forming process, and kinematic validation of the operating sequence. The Solidworks platform (thermal study), ANSYS Workbench (Polyflow Classic module), and the Unity 3D development environment were used for system integration.

#### 3.1. THERMAL VALIDATION OF HEATING SYSTEM (SOLIDWORKS)

The objective of this study was to verify the temperature uniformity on the PET sheet and the energy efficiency of the oven. A control volume was defined that included the quartz heaters, the reflective walls, and the target polymer. Due to the absence of predefined libraries for specific components, custom materials were configured in the preprocessor.

**Reflectors (Oven Body):** A polished 6061 aluminum alloy was modeled. A high thermal reflectivity ( $\sim 95\%$ ) and a reduced emissivity of  $\epsilon = 0.1$  were assigned in order to maximize the radiation incident on the material and minimize losses to the outside. A thermal conductivity  $k$  in the range of  $160 - 200 \text{ W/m} \cdot \text{K}$  was considered to avoid localized hot spots.

**Heating Elements:** The resistors were defined with quartz properties, assigning an internal heat generation power of  $400 \text{ W}$  per element as previously mentioned.

**PET Sheet:** An emissivity of  $\epsilon = 0.9$  was assigned on the face exposed to radiation, a characteristic value for the thermal absorption of thermoplastic polymers.

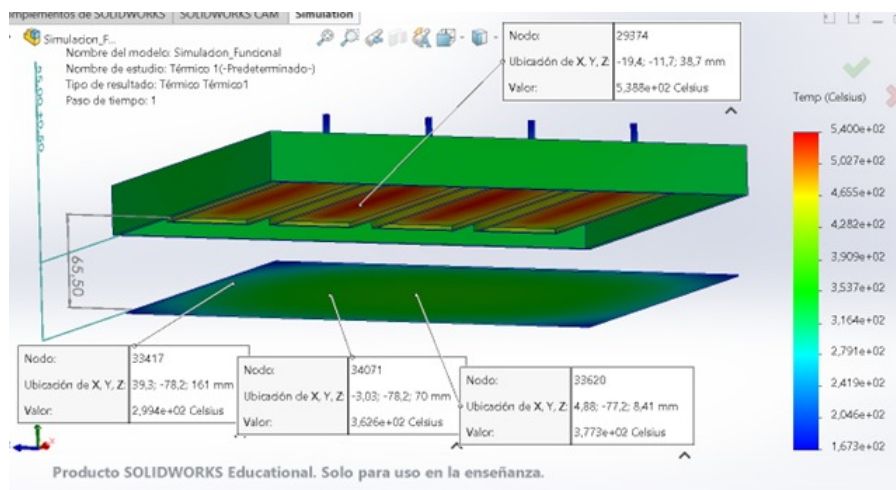
The analysis was configured as a steady-state surface-to-surface radiation problem. Environmental conditions were established by simulating a standard industrial building:

**Table 3.1.** Mean surface temperature and power density for Standard FQE range [5]

Power (W)	Mean Surface Temperature (°C)	Max Power Density (kW/m <sup>2</sup> )
250 W	438	15
400 W	542	24
500 W	593	30
650 W	664	39
750 W	690	45
1000 W	772	60

- Ambient temperature:  $T_{amb} = 20 \text{ °C}$ .
- Convection coefficient: A conservative coefficient of  $h = 5 \text{ W/m}^2 \cdot \text{K}$  was applied, assuming natural convection in a closed environment, which validates that radiation is the predominant energy transfer mechanism.

Initially, the system was evaluated under steady-state conditions to verify the heating capacity of the resistors. As shown in Figure 3.1, the heat on the sheet is distributed uniformly. The simulation corroborated the manufacturer's data, where the sized 400 W heaters reach an average  $T$  surface temperature of 542 °C.

**Figure 3.1.** Steady state analysis

However, the simulation indicated that, under prolonged exposure (steady state), the sheet would reach temperatures between 350-370 °C. These values are atypical and excessive for the thermoforming process, as they would degrade the material, leading

it to a viscous/liquid state. Therefore, it is concluded that process control should be strictly governed by transient exposure times and not by thermal equilibrium.

### 3.1.1. Transient State Analysis and Heating Curves

To determine the actual heating time, a transient simulation was configured with a total time of 600 s and sampling intervals of 60 s. The objective was to identify the moment when the sheet reaches the thermoforming temperature (115-140 °C). Three scenarios were evaluated by varying the distance between the emitter and the receiver, and the initial conditions

### 3.1.2. TEST 1 (Distance 65 mm - Cold Start)

Test 1 (Distance 65 mm - Cold Start): With a separation of 65 mm, the central nodes of the sheet took between 340 and 360 s to reach the target temperature. The edges of the sheet did not reach the glass transition temperature within this timeframe, indicating in Figure 3.2 the inefficiency in heat transfer under these conditions .

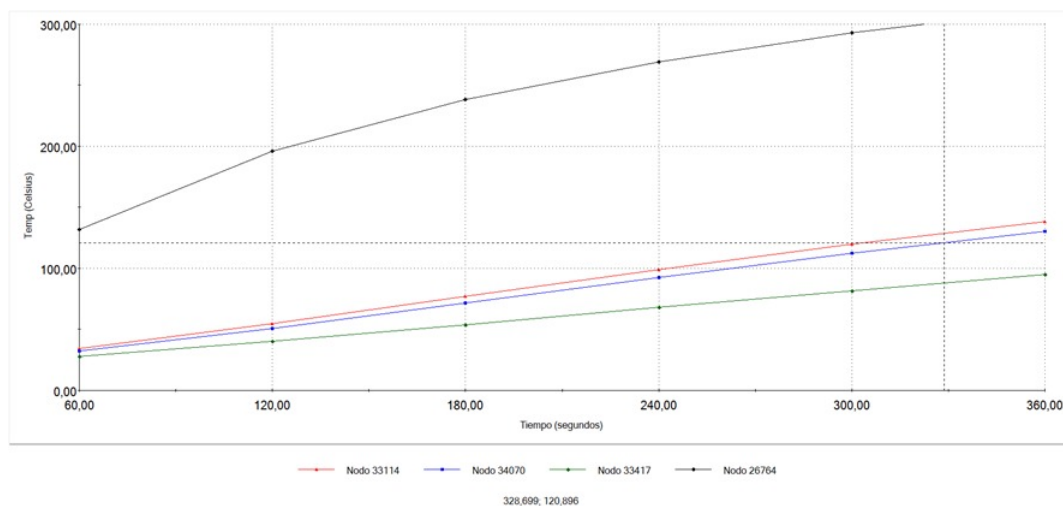


**Figure 3.2.** PET Sheet and Heater temperatures at a distance of 65mm

### 3.1.3. TEST 2 (Distance 40 mm - Cold Start)

By reducing the distance to 40 mm (less than the 5 cm recommended by the manufacturer, but adjusted for optimization), the time was reduced. The central nodes

reached the forming temperature between 280 and 300 s. However, as shown in Figure 3.3, the quartz resistor had not yet reached its nominal temperature during this period, remaining close to 300 °C.

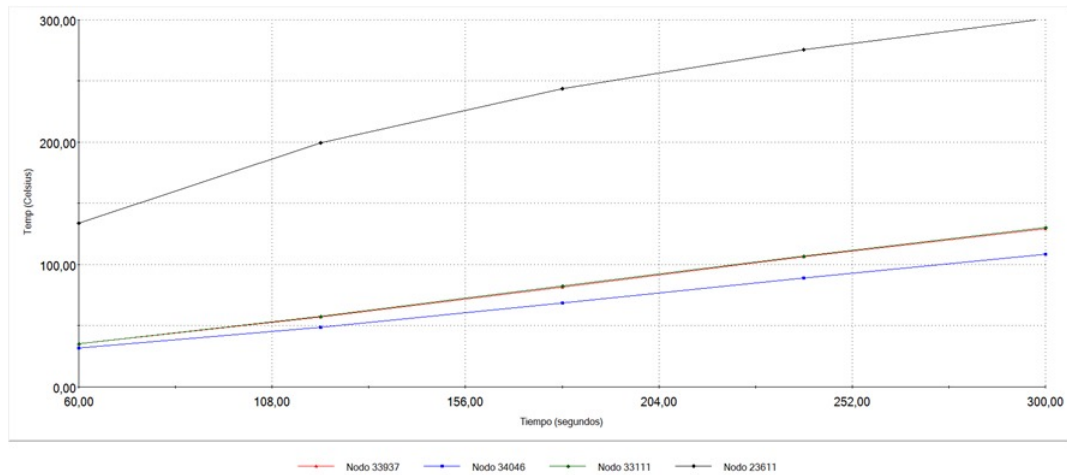


**Figure 3.3.** PET Sheet and Heater temperatures at a distance of 40mm

### 3.1.4. TEST 3 (PREHEATING)

The process shown in Figure 3.4 was simulated assuming that the quartz resistors were already at their nominal operating temperature (542 °C) when the sheet was introduced. Under this condition, the PET sheet reached the forming temperature in less than 30 seconds.

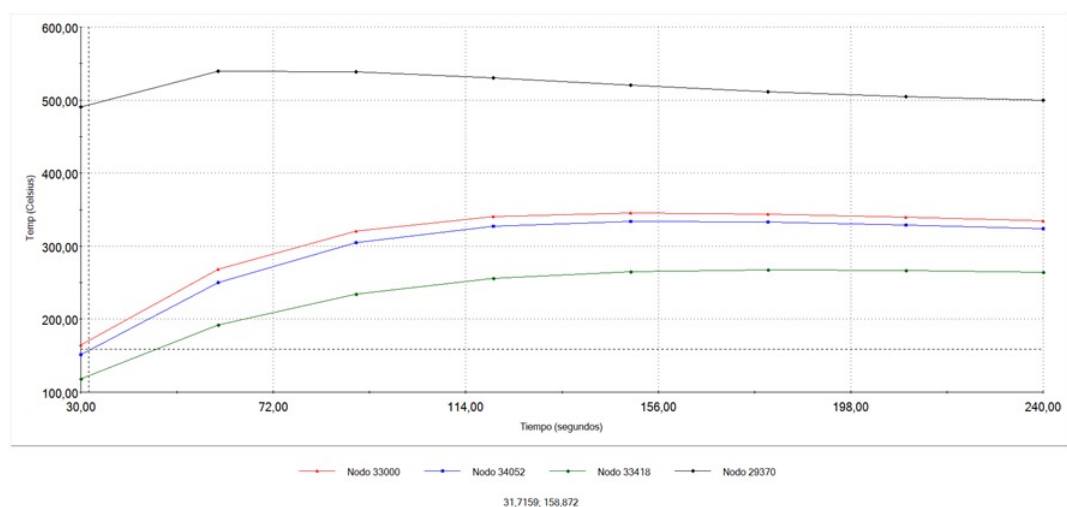


**Figure 3.4.** PET Sheet and Heater temperatures with initial working temperature of Quartz elements

This final test illustrated in Figure 3.5 validates that, in order to meet the estimated production cycles, the machine must operate with a preheating system or keep the heating elements on between cycles, allowing for fast forming times in accordance with the design.

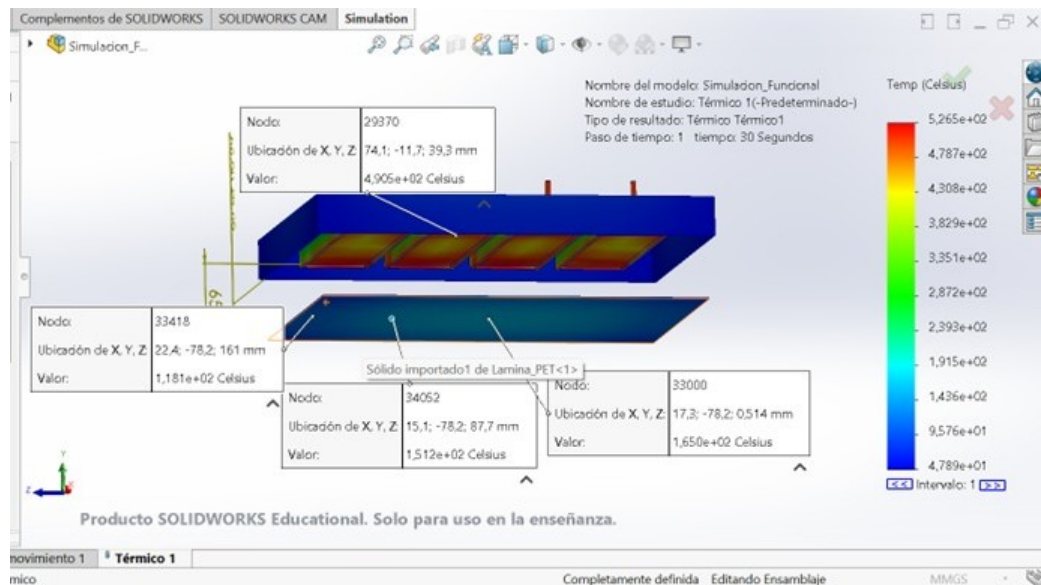


**Figure 3.5.** Transient State Analysis

### 3.2. THERMOFORMING PROCESS SIMULATION(ANSYS)

To evaluate the material's behavior during molding, the ANSYS Polyflow solver, specialized in polymer flows and large deformations, was used.

**A. Discretization and Meshing:** An adaptive mesh was generated on the surface of the PET sheet and the mold geometry. Due to computational node restrictions in the academic license used, a simplification of the mold topology was applied, prioritizing mesh refinement in the areas of greatest curvature where the greatest material stretching is expected.

**B. Process Parameters:** The model was configured as a vacuum forming process, defining the following interaction parameters:

- **Vacuum Pressure:** A differential pressure of 91400 Pa (approx. 90% absolute vacuum) was applied, corresponding to the capacity of the selected vacuum pump (27 inHg).

- **Constraints:** Zero displacement boundary conditions were applied to the edges of the sheet, simulating the mechanical action of the clamping frame.
- **Cycle Time:** The deformation interaction was evaluated in a time window of 1.5 s, coinciding with the vacuum application phase.

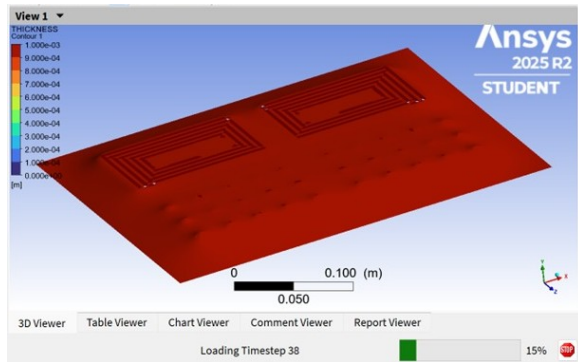
The results, presented in Figure 3.6, show the thickness distribution after forming. Maximum stretching is observed on the vertical walls of the mold (areas of greater tension), represented in yellow/orange. The faces opposite the base of the mold and the settling areas maintain an optimal thickness of between 0.9 and 1.0 mm.

This distribution is favorable for the application of egg cartons by its structural integrity, as it maintains rigidity at the vertices and the base, critical areas to avoid fractures due to impact or handling. It is important to note that the design considered the Plastiglas guidelines, assuming a shrinkage of 2% in both directions and a thermal contraction of 0.6% to 1% upon cooling. It should be mentioned that the simulation did not consider thermal variations of the material during deformation (simplified isothermal process), which could slightly influence the definition of minor details such as the closing ribs.

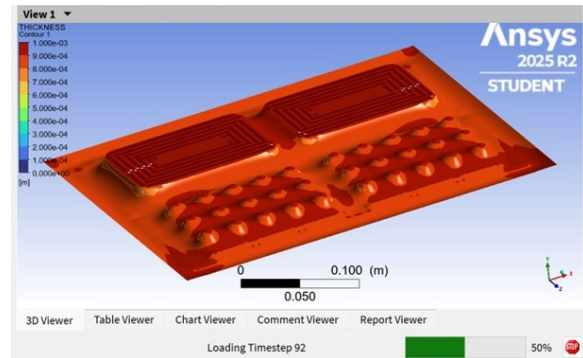
### 3.3. KINEMATIC AND SEQUENTIAL VALIDATION (UNITY 3D)

A preliminary prototype was developed in the Unity environment to validate the control logic, collision detection, and machine cycle times. The geometry was imported in OBJ format from Autodesk Inventor. The flowchart shown in Figure 2.4 was used as a guide for the cycle.

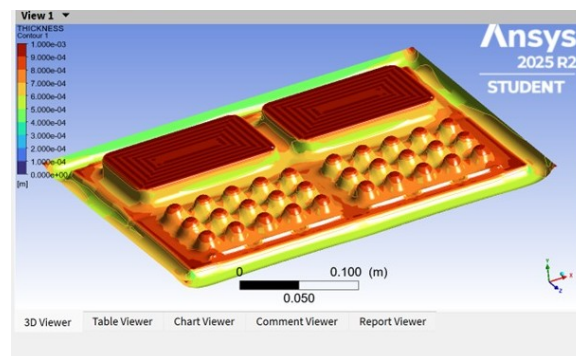
Each component (pistons, frame, plate) was assigned physical properties (Rigid Body, Mesh Collider) and hierarchical relationships. The kinematics of the pneumatic actuators were programmed using C# scripts, employing analytically calculated velocities to ensure physical realism.



(a) STAGE 1-Contact between PET sheet and mold



(b) STAGE 2- Vacuum application



(c) STAGE 3- Thermoformed sheet

Figure 3.6. PET Sheet thickness in vacuum forming

### 3.3.1. Pneumatic Actuation Calculation

To ensure the simulation reflected realistic dynamics, the velocity of the pneumatic cylinders was calculated analytically rather than arbitrarily assigned. Considering a system pressure ( $P$ ) of 4 bar and a required force ( $F$ ) of 45.2 N, the effective piston area ( $A$ ) was verified as:

$$A = \frac{F}{P} = \frac{45.2 \text{ N}}{4 \times 10^5 \text{ Pa}} \approx 1.13 \times 10^{-4} \text{ m}^2 \quad (3.1)$$

This confirms a piston diameter of approximately 12 mm. Assuming a standard valve flow rate ( $Q$ ) of 60 NI/min ( $0.001 \text{ m}^3/\text{s}$ ), the theoretical maximum velocity ( $v_{\text{th}}$ ) is:

$$v_{\text{th}} = \frac{Q}{A} = \frac{0.001 \text{ m}^3/\text{s}}{1.13 \times 10^{-4} \text{ m}^2} \approx 8.85 \text{ m/s} \quad (3.2)$$

However, for operational safety and process control, flow regulation valves are em-

ployed. Consequently, the simulation velocity was set to a practical value of 0.3 m/s. The resulting cycle time ( $t$ ) for a 200 mm stroke is:

$$t = \frac{d}{v_{\text{prac}}} = \frac{0.2 \text{ m}}{0.3 \text{ m/s}} \approx 0.67 \text{ s} \quad (3.3)$$

This calculation validated the programmable logic controller (PLC) sequence, ensuring the machine achieves the target production rate of one tray per minute (including 30 s heating, forming, and ejection).

The simulation allows visualization of the process stages (loading, heating, forming, cooling, and ejection) in real time, as can be observed in Figure 3.7. The coordination of the pneumatic cylinders movement and the stable clamping of the sheet metal by the frame were validated.

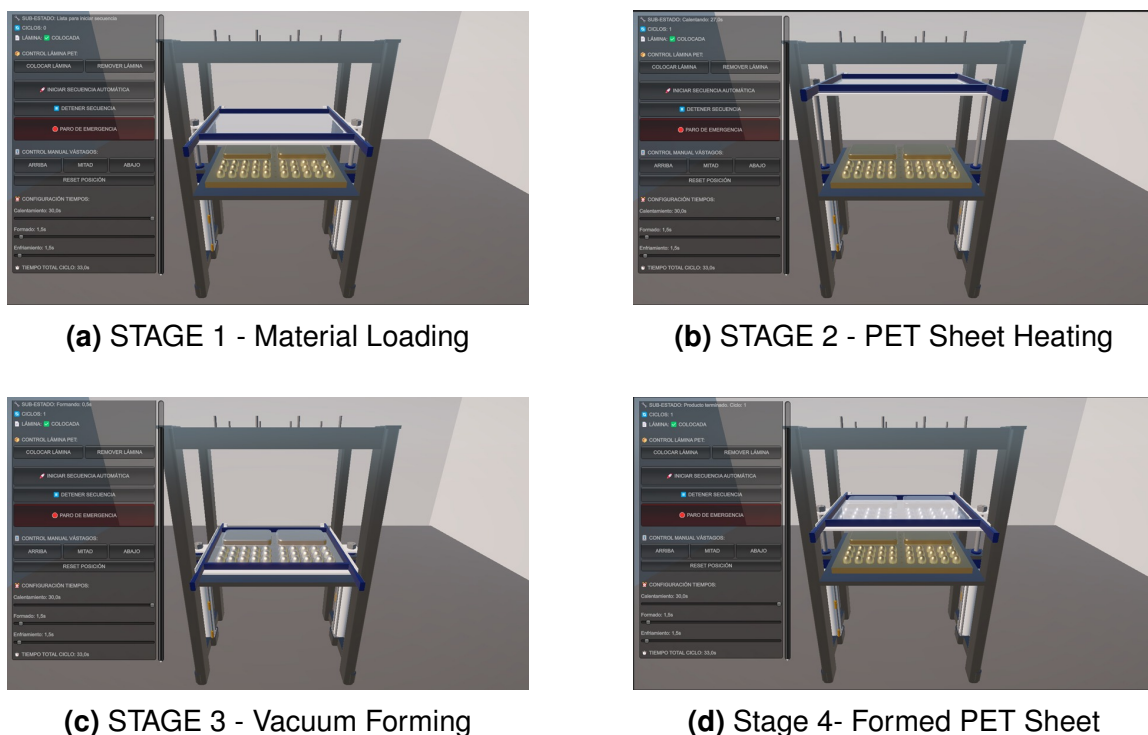


**Figure 3.7.** Thermoforming machine sequence

The sequence in Unity corresponds to the logic programmed in a Ladder diagram (see Appendix ), validating the PLC's inputs (limit switches, emergency stop button, start) and outputs. The virtual environment confirms that the spatial arrangement of the structural elements is correct and that the kinematics of the mechanism meet the design

constraints, demonstrating that the prototype is functional, compact and scalable for different forming matrices.

## Chapter 4

### CONCLUSIONS AND RECOMMENDATIONS

#### 4.1. CONCLUSIONS

Heat transfer analysis confirmed that the 400 W resistor configuration ensures uniform heat distribution. Transient studies determined a preheating time of 30 s, achieving a balance between the thermal inertia of PET and energy savings.

The designed vacuum system reached the necessary pressure levels to ensure the geometric replicability of the mold. The suction flow was verified to maintain the structural integrity of the egg tray, resulting in consistent wall thicknesses between 0.7 and 1.0 mm.

The mechanical architecture were validated in a virtual environment to achieve precise synchronization of the pneumatic and thermal stages.

Functional tests on the virtual prototype demonstrated the technical feasibility of the integrated system, satisfactorily meeting design standards and enabling parallel production of two units per cycle without spatial collisions.

In conclusion an automated manufacturing system was successfully consolidated, integrating mechanical design, pneumatics, and thermal system, ensuring a continuous and efficient production flow for the manufacture of plastic buckets.

#### 4.2. RECOMMENDATIONS

For the subsequent physical implementation phase, it is proposed to integrate a closed-loop PID control system . This hardware integration is essential to stabilize the quartz emitter temperature at its nominal operating setpoint of 542 °C for cycle start.

To facilitate operation and diagnostics, it is recommended to develop a graphical interface (HMI). This would allow for real-time visualization of temperatures, pressures, actuator status, and cycle counters, as well as enabling safe parameter adjustments.

It is essential to establish a preventive maintenance plan for pneumatic actuators and solenoid valves. In addition to using filtered and lubricated air, to detect wear or synchronization failures early.

To increase robustness, the integration of a vision camera could be explored. This would allow for verification, before molding, of the correct position, temperature and presence of the PET sheet, preventing empty cycles or potential damage to the mold.

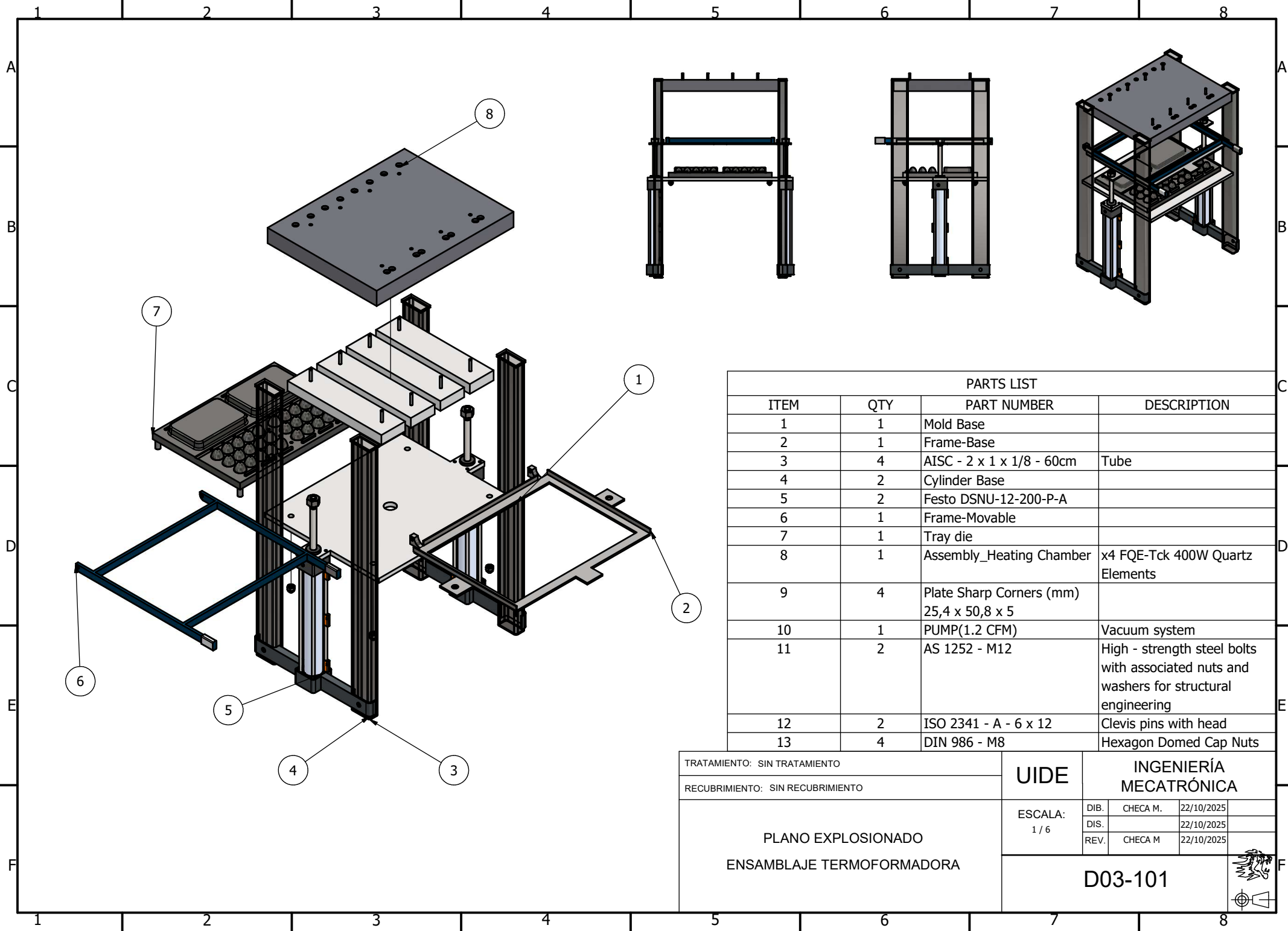
## REFERENCES

- [1] G. Aultman, "The thermoforming process explained," VANTAGE Plastics, n.d., accessed via Vantage Plastics website.
- [2] J. Rosales-Dávalos, L. Gil-Antonio, J. E. Mastache-Mastache, y R. López-Ramírez, "Diseño e implementación de un sistema de control a lazo cerrado PID para manipular la temperatura en el proceso de termoformado," *Revista de Ingeniería Eléctrica*, vol. 4, no. 12, pp. 24–29, Jun 2020.
- [3] FESTO, "ISO cylinder." [En línea]. Disponible: <https://www.festo.com/us/en/a/19196/>
- [4] EUROTECH Vacuum Technologies, "¿Qué es el vacío? Conceptos básicos y aplicaciones," 9 2025, consultado: 15 de octubre de 2024. [En línea]. Disponible: <https://eurotech-vacuum-technologies.com/es/what-is-vacuum/>
- [5] C. Ltd, "Elemento de cuarzo completo (FQE) - Ceramicx," 1 2026. [En línea]. Disponible: <https://www.ceramicx.com/es/products/quartz-elements/standard-quartz-elements/full-quartz-element/>
- [6] S. Engelmann, *Advanced Thermoforming: Methods, Machines and Materials, Applications, Automation, Sustainability, and the Circular Economy*. Hoboken, NJ: John Wiley & Sons, Inc., 2023.
- [7] *Manual de Termoformado*, Plastiglas, CDMX, 2020, [Online]. Available: [https://www.plastiglas.com.mx/pdfs/literatura/Manual\\_termoformado.pdf](https://www.plastiglas.com.mx/pdfs/literatura/Manual_termoformado.pdf). [En línea]. Disponible: <https://www.plastiglas.com.mx>
- [8] C. Aiña, "Desarrollo de un sistema de control automático de temperatura para el horno de calentamiento de máquinas de termoformado," Tesis de maestría, Universidad Politécnica Salesiana, Quito, Ecuador, Feb 2025. [En línea]. Disponible: <https://dspace.ups.edu.ec/bitstream/123456789/29501/1/TTS2085.pdf>

- [9] L. Miranda y A. Zacasari, "Diseño de una máquina termoformadora para la elaboración de piezas plásticas," Tesis de maestría, Universidad Politécnica Salesiana, Cuenca, Ecuador, Jan 2023. [En línea]. Disponible: <http://dspace.ups.edu.ec/handle/123456789/24355>
- [10] E. Malavé y J. Tigrero, "Fabricación de máquina de moldeo por termocompresión para elaborar paneles plásticos como material de construcción," Tesis de maestría, Universidad Estatal Península de Santa Elena (UPSE), La Libertad, Ecuador, 2025. [En línea]. Disponible: <https://repositorio.upse.edu.ec/handle/46000/12520>
- [11] I. Morán y B. Laica, "Diseño e implementación de un sistema de control y monitoreo de temperatura en hornos eléctricos para la quema de cerámica en los laboratorios de diseño gráfico," Tesis de maestría, Escuela Superior Politécnica de Chimborazo (ESPOCH), Riobamba, Ecuador, 2024.
- [12] OMEGA, "Electric tubular heaters," 2025, [Online; accessed 02-Aug-2025]. [En línea]. Disponible: <https://www.omega.co.uk/prodinfo/tubular-heaters.html>
- [13] W. Tupia, L. E. B. Haro, A. Arribasplata, y J. Acosta, "Metodología experimental para determinar los parámetros del proceso de moldeo por compresión de materiales compuestos de termoplástico reciclado y madera recuperada," *Matéria (Rio de Janeiro)*, vol. 25, no. 3, 2020.
- [14] R. G. Bernal, C. A. Z. Guerrero, J. J. P. Castillo, J. C. T. Jiménez, y F. I. T. Reyes, "Diseño de prensa hidráulica para reciclar polietileno de alta densidad (HDPE) en forma de placas," *Ciencia Nicolaita*, no. 86, Dec 2022.
- [15] S. R. Rosen, *Thermoforming: Improving Process Performance*. Society of Manufacturing Engineers, 2002.
- [16] R. Vaca, "Fabricación de una máquina de termoformado para el laboratorio de procesamiento de plásticos," Tesis de maestría, Escuela Superior

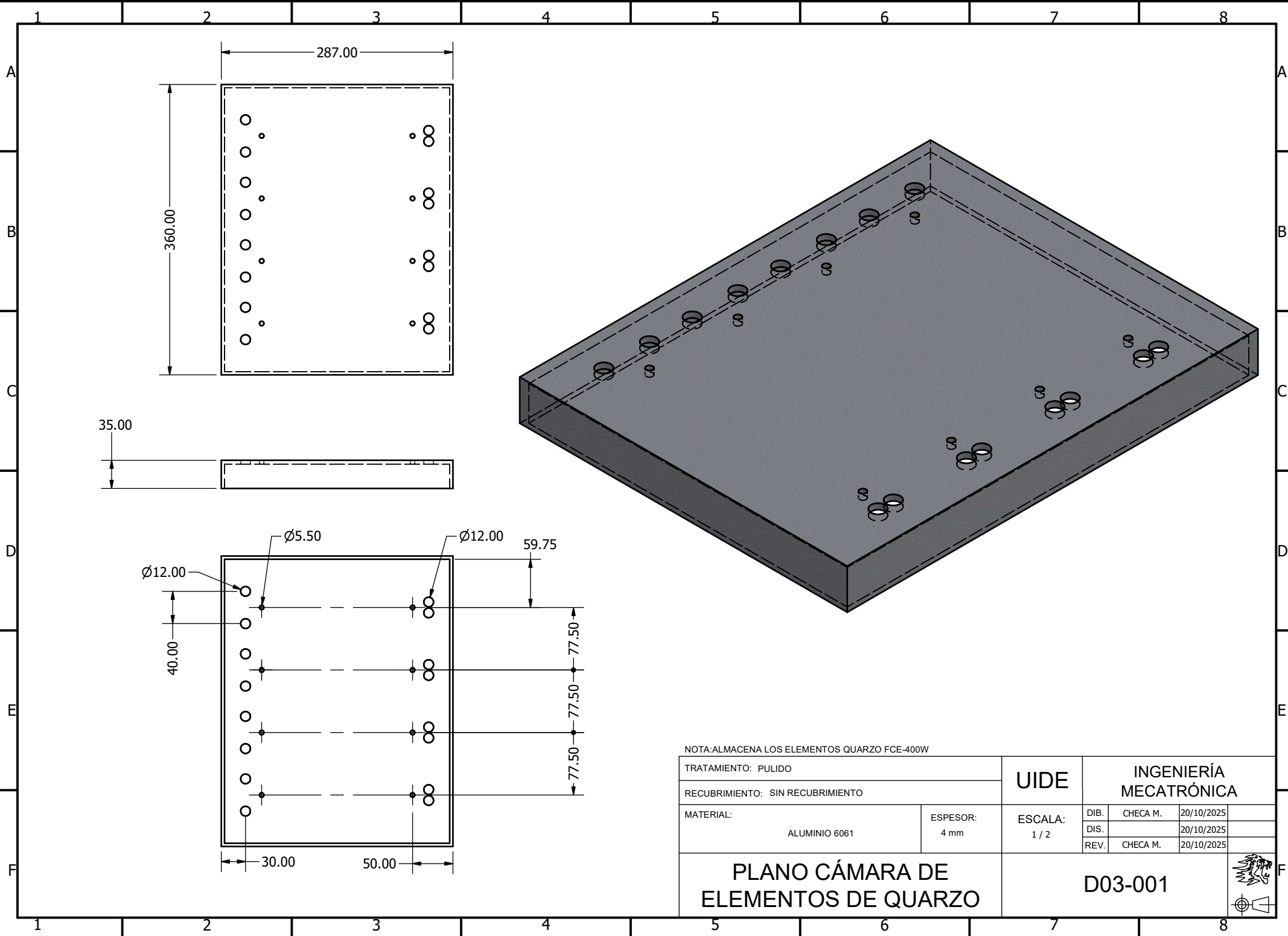
Politécnica del Litoral (ESPOL), Quito, Ecuador, 2022. [En línea]. Disponible: <http://www.dspace.espol.edu.ec/handle/123456789/57338>

- [17] N. Banús, I. Boada, P. Xiberta, P. Toldrà, y N. Bustins, “Deep learning for the quality control of thermoforming food packages,” *Scientific Reports*, vol. 11, no. 1, p. 21887, Nov 2021.
- [18] E. Turan *et al.*, “Digital twin modelling for optimizing the material consumption: A case study on sustainability improvement of thermoforming process,” *Sustainable Computing: Informatics and Systems*, vol. 35, p. 100655, Sep 2022.
- [19] R. Cortez, J. Martínez, y F. Donis, “Los métodos experimentales y su importancia en la enseñanza de la ingeniería mecánica como complemento al diseño asistido por computadora,” *Ciencia, Tecnología y Humanidades*, Jun 2021.
- [20] S. Mishra y A. V. Ullas, “Concept modelling of small scale device for continuous production of graphene using SolidWorks,” *Materials Today: Proceedings*, vol. 79, pp. 345–348, 2023.
- [21] G. P. Monizza, I. D. Blasio, y D. T. Matt, “Exploring applications of computational design techniques and design for manufacturability for costs reduction of prefabricated timber-based façades: The ‘legnattivo’ design prototype,” *Developments in the Built Environment*, vol. 19, p. 100489, Oct 2024.
- [22] R. Abdallah *et al.*, “The use of SolidWorks in the evaluation of wind turbines in palestine,” *Energy Nexus*, vol. 7, p. 100135, Sep 2022.
- [23] Y. Chen, G. Quino, y A. Pellegrino, “A comprehensive investigation on the temperature and strain rate dependent mechanical response of three polymeric syntactic foams for thermoforming and energy absorption applications,” *Polymer Testing*, vol. 130, p. 108287, Jan 2024.
- [24] Olam, Mikail, “Pet: Production, properties and applications,” pp. 131–162, 11 2021.



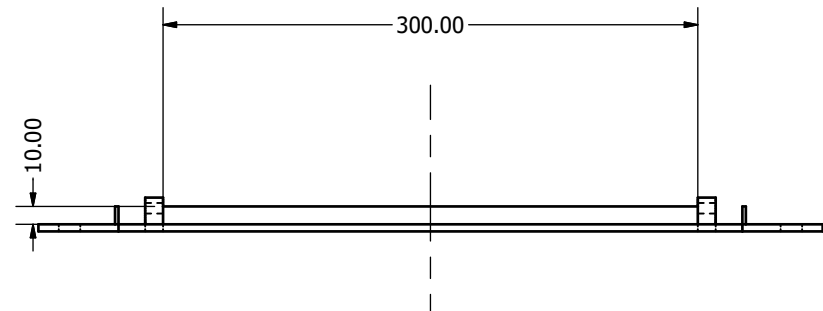
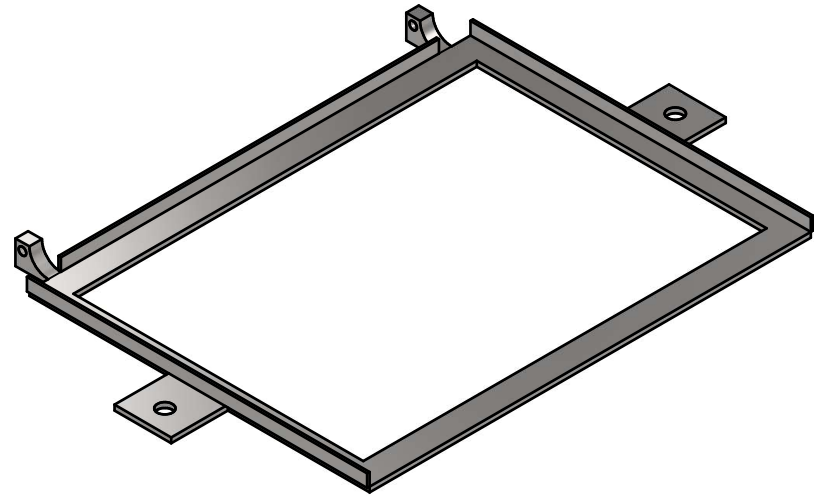
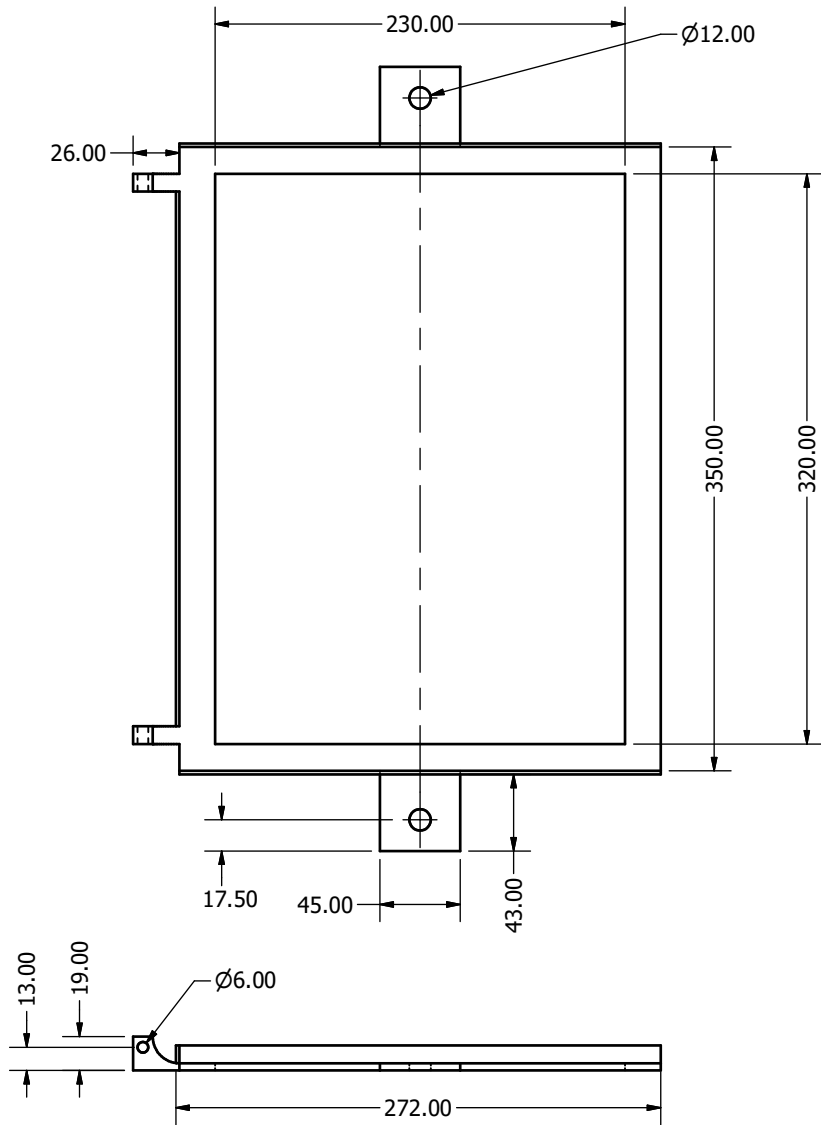
PARTS LIST			
ITEM	QTY	PART NUMBER	DESCRIPTION
1	1	Mold Base	
2	1	Frame-Base	
3	4	AISC - 2 x 1 x 1/8 - 60cm	Tube
4	2	Cylinder Base	
5	2	Festo DSNU-12-200-P-A	
6	1	Frame-Movable	
7	1	Tray die	
8	1	Assembly_Heating Chamber	x4 FQE-Tck 400W Quartz Elements
9	4	Plate Sharp Corners (mm) 25,4 x 50,8 x 5	
10	1	PUMP(1.2 CFM)	Vacuum system
11	2	AS 1252 - M12	High - strength steel bolts with associated nuts and washers for structural engineering
12	2	ISO 2341 - A - 6 x 12	Clevis pins with head
13	4	DIN 986 - M8	Hexagon Domed Cap Nuts

TRATAMIENTO: SIN TRATAMIENTO		<b>UIDE</b>	<b>INGENIERÍA MECATRÓNICA</b>	
RECUBRIMIENTO: SIN RECUBRIMIENTO			DIB.	CHECA M.
<b>PLANO EXPLOSIONADO</b> <b>ENSAMBLAJE TERMOFORMADORA</b>		ESCALA:		
		1 / 6	DIS.	22/10/2025
		REV.	CHECA M	22/10/2025
		<b>D03-101</b>		

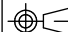


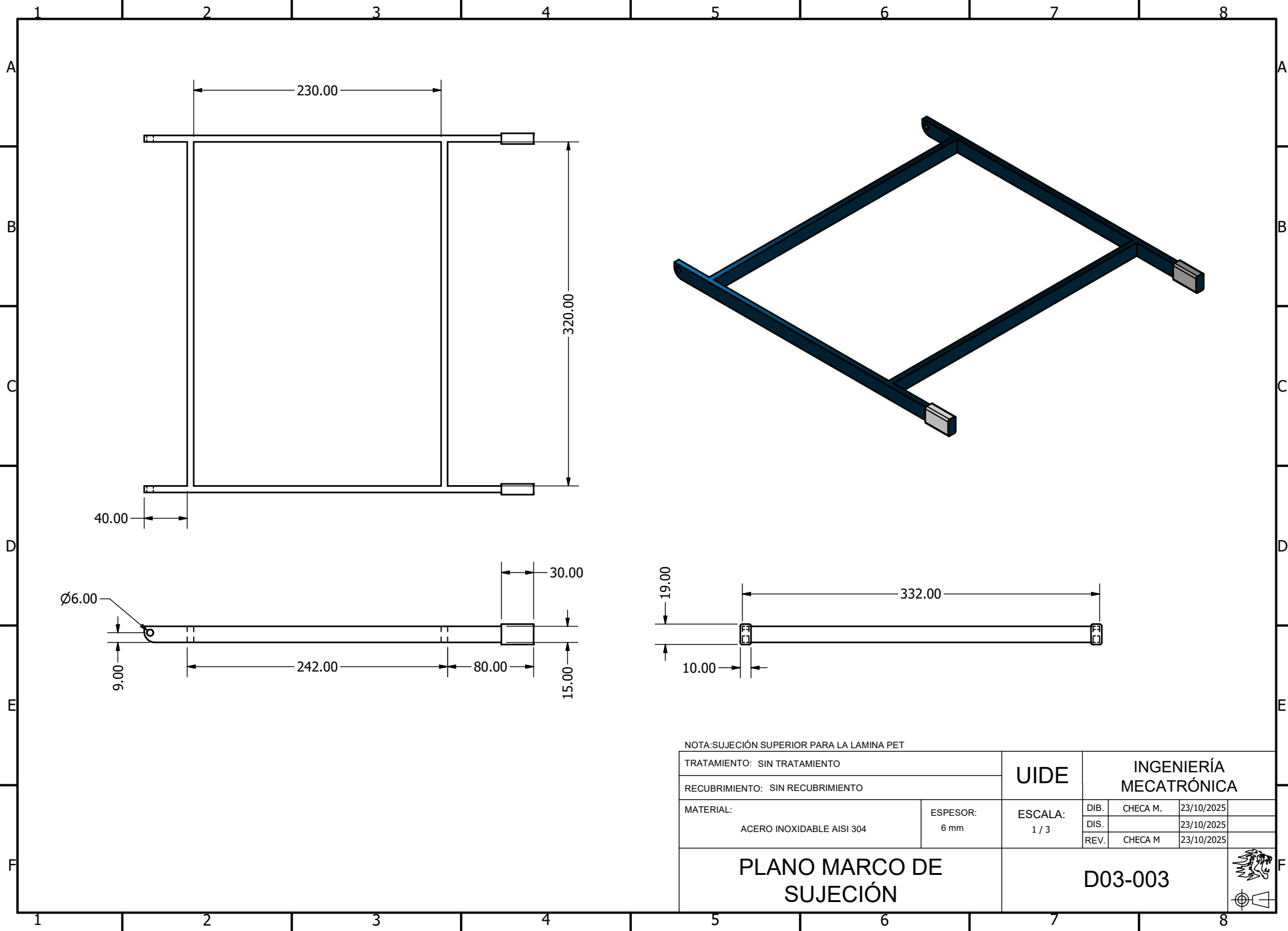
NOTA:ALMACENA LOS ELEMENTOS QUARZO FCE-400W

TRATAMIENTO: PULIDO		UIDE	INGENIERÍA MECATRÓNICA		
RECUBRIMIENTO: SIN RECUBRIMIENTO			DIB.	CHECA M.	20/10/2025
MATERIAL:  ALUMINIO 6061	ESPESOR: 4 mm	ESCALA:	1 / 2		
		DIS.	20/10/2025		
		REV.	CHECA M. 20/10/2025		
PLANO CÁMARA DE ELEMENTOS DE QUARZO		D03-001			



NOTA: SOPORTE PARA LA LAMINA PET

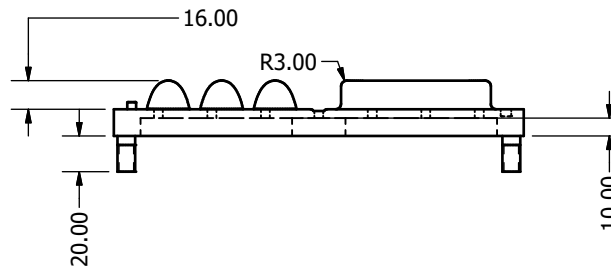
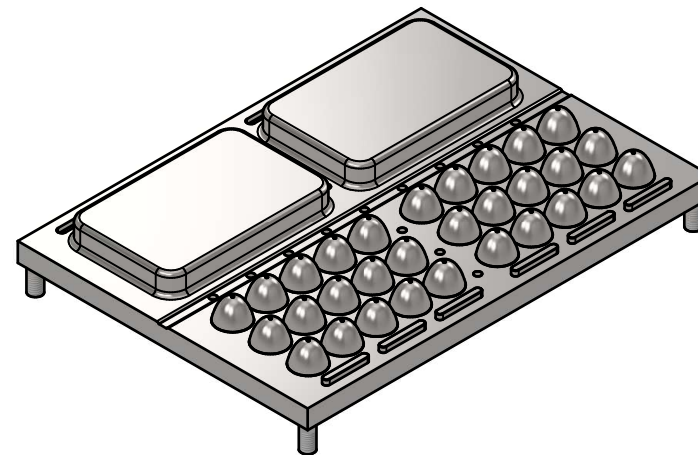
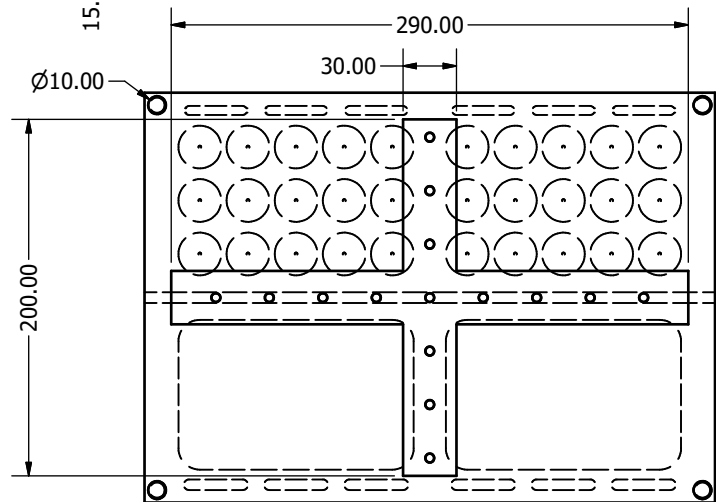
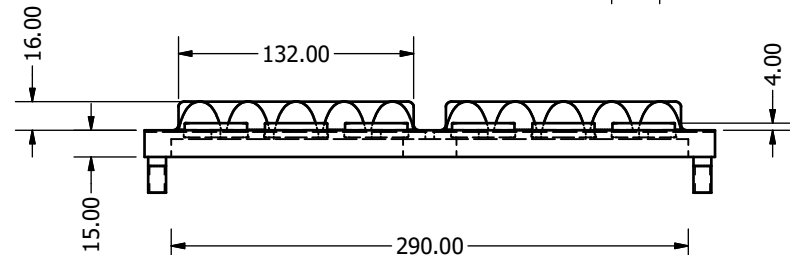
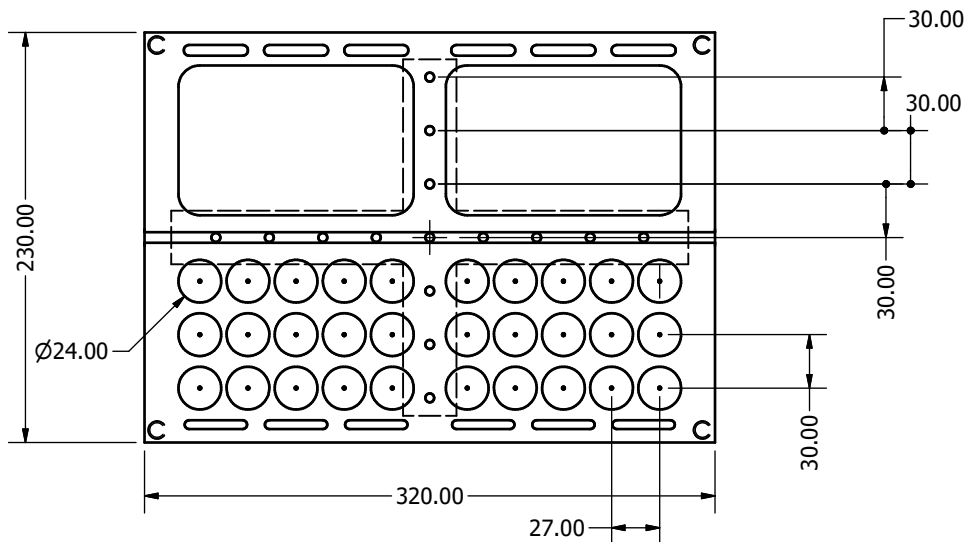
TRATAMIENTO: SIN TRATAMIENTO		UIDE	INGENIERÍA MECATRÓNICA		
RECUBRIMIENTO: SIN RECUBRIMIENTO			DIB.	CHECA M.	23/9/2025
MATERIAL: ACERO INOXIDABLE AISI 304		ESPAESOR: 4 mm	ESCALA: 1 / 3	DIS.	23/9/2025
			REV.	CHECA M	23/9/2025
PLANO MARCO BASE			D03-002		



NOTA: SUJECIÓN SUPERIOR PARA LA LAMINA PET

TRATAMIENTO: SIN TRATAMIENTO		UIDE	INGENIERÍA MECATRÓNICA		
RECUBRIMIENTO: SIN RECUBRIMIENTO			DIB.	CHECA M.	23/10/2025
MATERIAL: ACERO INOXIDABLE AISI 304		ESPELOR: 6 mm	ESCALA: 1 / 3	DIS.	23/10/2025
			REV.	CHECA M	23/10/2025
<b>PLANO MARCO DE SUJECIÓN</b>			<b>D03-003</b>		

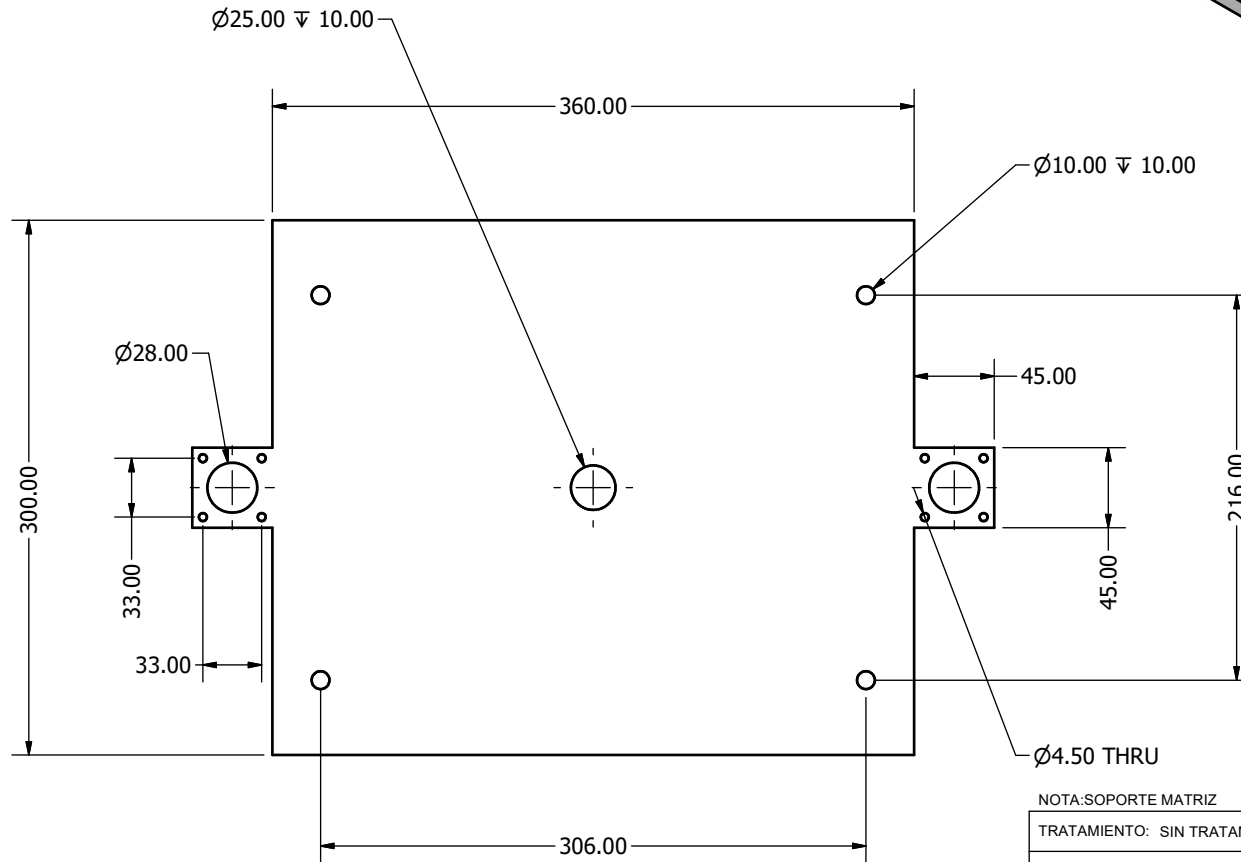
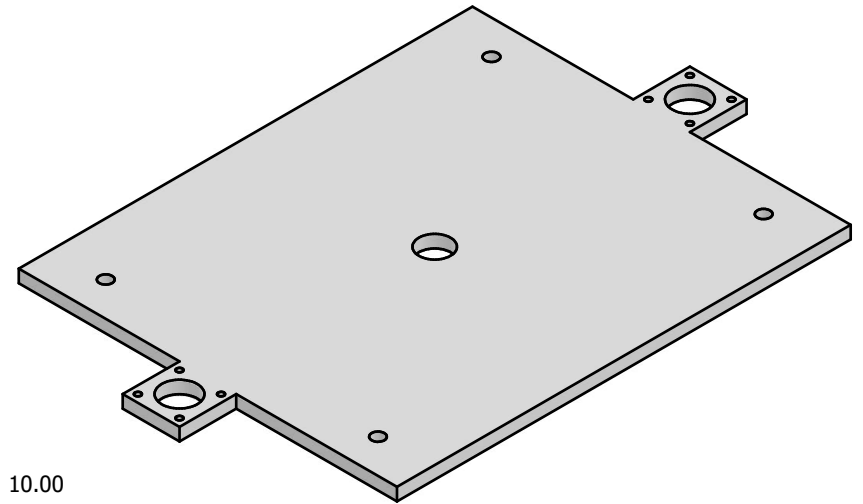
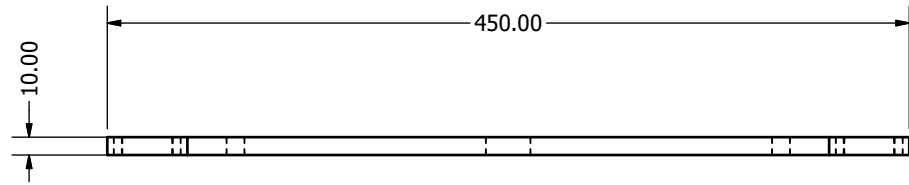




NOTA: MATRIZ PARA LA LAMINA PET

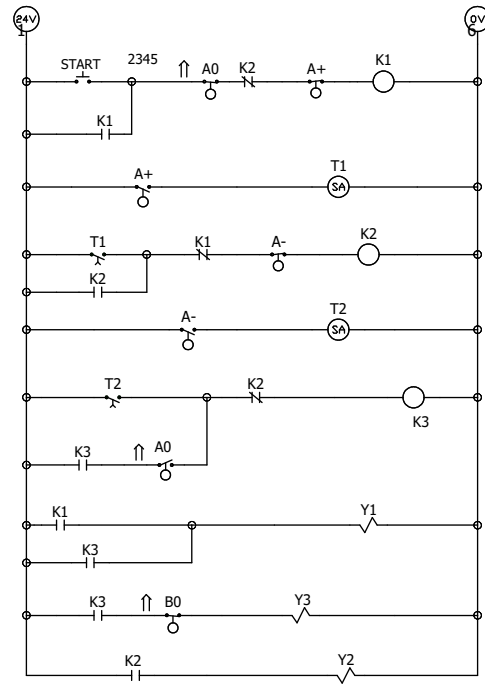
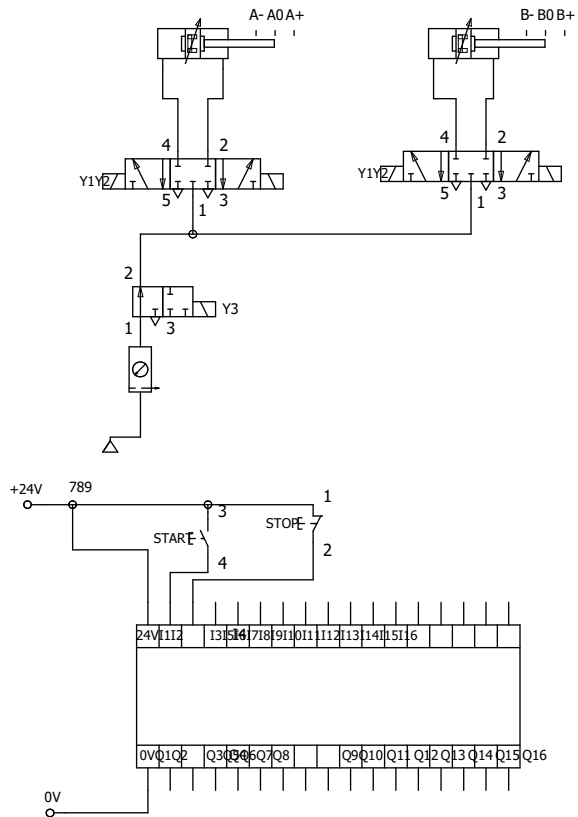
TRATAMIENTO: SIN TRATAMIENTO		UIDE	INGENIERÍA MECATRÓNICA		
RECUBRIMIENTO: SIN RECUBRIMIENTO			DIB.	CHECA M.	29/9/2025
MATERIAL:	ESPELOR:	ESCALA:	DIS.	29/9/2025	
ALEACION ALUMINIO 6061		1 / 3	REV.	CHECA M	29/9/2025
PLANO MOLDE CUBETA			D03-004		





NOTA: SOPORTE MATRIZ		UIDE	INGENIERÍA MECATRÓNICA		
TRATAMIENTO: SIN TRATAMIENTO			ESCALA: 1 / 3	DIB.	CHECA M.
RECUBRIMIENTO: SIN RECUBRIMIENTO		DIS.			13/10/2025
MATERIAL: ALEACION ALUMINIO 6061		ESPESOR: 10mm		REV.	CHECA M
PLANO BASE MOLDE			D03-005		





UIDE	INGENIERÍA MECATRÓNICA	
	DIB. CHECA M.	01/01/2026
	DIS.	
REV. CHECA M	01/01/2026	

PLANO ELECTRONEUMÁTICO

D01-001

